

# Anomalous diffusion originated by two Markovian hopping-trap mechanisms

S Vitali<sup>1</sup>, P Paradisi<sup>1,2</sup>, G Pagnini<sup>1,3</sup>

<sup>1</sup> BCAM–Basque Center for Applied Mathematics, Alameda de Mazarredo 14, E-48009 Bilbao, Basque Country - Spain

<sup>2</sup> ISTI–CNR, Institute of Information Science and Technologies "A. Faedo", Via Moruzzi 1, I-56124 Pisa, Italy

<sup>3</sup> Ikerbasque–Basque Foundation for Science, Plaza Euskadi 5, E-48009 Bilbao, Basque Country - Spain

E-mail: [gpagnini@bcamath.org](mailto:gpagnini@bcamath.org)

Original Submission: 27 October 2021

Revised version: 11 April 2022

**Abstract.** We show through intensive simulations that the paradigmatic features of anomalous diffusion are indeed the features of a (continuous-time) random walk driven by two different Markovian hopping-trap mechanisms. If  $p \in (0, 1/2)$  and  $1 - p$  are the probabilities of occurrence of each Markovian mechanism, then the anomalousness parameter  $\beta \in (0, 1)$  results to be  $\beta \simeq 1 - 1/\{1 + \log[(1 - p)/p]\}$ . Ensemble and single-particle observables of this model have been studied and they match the main characteristics of anomalous diffusion as they are typically measured in living systems. In particular, the celebrated transition of the walker's distribution from exponential to stretched-exponential and finally to Gaussian distribution is displayed by including also the Brownian yet non-Gaussian interval.

Submitted to: *J. Phys. A: Math. Theor.*

## 1. Introduction

We show that anomalous diffusion emerges from a process that goes through the action of two *co-existing* Markovian mechanisms acting with different statistical frequency. In other words, anomalous diffusion emerges from standard diffusion when very seldomly the process switches to another standard diffusion with a different set-up: the probability of occurrence of this switch originates and fully characterizes the anomalous diffusion such that anomalous diffusion is indeed not originated by a broad distribution of relaxation times [1, 2], or by a crowded environment [3], or by other mechanisms linking it to complexity [4].

The motion of a random walker is called diffusion when it goes through a dissipative evolution and the ensemble statistics of the process are characterized by the convergence of the walker's probability density function (PDF) to the Gaussian distribution and also by a mean-square displacement (MSD) that is linear in time, namely the Brownian motion (Bm). An offspring of the Gaussianity and of the Bm is that the governing equation of the walker's PDF, i.e., the Fokker–Planck (FP) equation, is an equation with a single and constant coefficient, that is the diffusion coefficient. Since the Gaussian distribution is also named Normal distribution, we have that the term diffusion turns into normal diffusion and whenever one, or both, of the characteristic features of the ensemble statistics of the normal diffusion are not fulfilled then the corresponding process falls into the class of the anomalous diffusion.

We study here anomalous diffusion as it emerges from over-damped processes only. In this respect, we report in this introductory section, as an overview, that the random walk for normal diffusion goes through the Galton board setting, namely, at each fixed time-step the walker performs a jump drawn from a symmetric distribution with finite variance [5]. But theories of random walks could be even very refined. So when, few decades ago, anomalous diffusion caught the attention of the scientific community "Random walks were an old topic that seemed fully understood and explored, belonging to textbooks and not having novel research directions" [6]. But, if the simple setting of the Galton board works well for normal diffusion with the assumption of independence between consecutive states, i.e., the Markovianity property, a fundamental feature of anomalous diffusion is embodied indeed by memory effects between consecutive states, i.e., the non-Markovianity property. Therefore the best candidate for modelling anomalous diffusion emerged to be the continuous-time random walk (CTRW), first introduced by Montroll and Weiss in 1965 [7]. Namely, the CTRW is a random walk which allows for random waiting-times between consecutive jumps and so there is no more a fixed time-step for time evolution but a time-step drawn by a distribution. As a matter of fact, this is a procedure for introducing non-Markovianity into the settings of the random walk. Later, many successes of the CTRW have been reported, see, e.g., [8, 9, 10, 11].

Anomalous diffusion took its place in 1973 when Scher and Lax discussed [12, 13], in general, transport processes in disordered systems, and, in particular, the diffusion

of carriers in amorphous semiconductor films for photocopying machines. In 1975 a successful model on the basis of the CTRW was proposed by Scher and Montroll [14] by using recent calculations in 1973 by Montroll and Scher [15] and in 1974 by Shlesinger [16]. 1973–1975 were anni mirabiles for the anomalous diffusion. After this, new applications of diffusion theory started to call for new modelling approaches and, by passing through a number of other applications in physics [17], anomalous diffusion landed nowadays in living systems [18, 19].

At the same time, the field of fractional calculus found its glorious application in modelling anomalous diffusion through the time-fractional generalisation of the diffusion equation, i.e., by replacing the first-order time-derivative with a non-local derivative operator of a fractional (actually a positive real) order. The link between anomalous diffusion and fractional calculus is embodied by the so-called memory effect that governs the diffusion and is encoded into the power-law kernel of the operators of fractional calculus. The story of fractional models for anomalous diffusion started in 1986 with Nigmatullin who modelled diffusion in porous medium by using fractal comb-like structures and come down to derive a time-fractional diffusion equation [20], see also reference [21] for other pioneering applications of fractional calculus. The same year, the solution to such equation was provided by Wyss [22] for a time fractional-order less than 1, that was extended to be less than 2 in 1989 by Schneider and Wyss [23]. Following Schneider and Wyss [23], in 1989, Nonnenmacher and Nonnenmacher applied fractional calculus to the Boltzmann equation for deriving a fractional extended irreversible thermodynamics [24], and in the same year Nonnenmacher [25] applied fractional calculus to lateral diffusion processes in biomembranes predicting the measured values more accurately than when being compared with the predictions of standard diffusion.

Later, in 1995–1996, Mainardi published noteworthy papers [26, 27, 28] where the time-fractional diffusion and its solution were put in an easy-to-understand setting that widely popularised the topic, for an historical summary we refer the reader to reference [29], and such popularisation continued with other noteworthy papers co-authored with Gorenflo, see, e.g., [30, 31, 32, 33]. Fractional diffusion were definitively legitimised in 2002 by Sokolov, Klafter and Blumen [34]. The meaning of time fractional-derivative in physical models was investigated since 1995 by Hilfer, see, among many, the papers [35, 36, 37, 38], and see also two critical analysis about the relation between fractional and fractality by Rutman dated 1994 and 1995 [39, 40]. The reader interested on the success of fractional calculus in anomalous diffusion can pass through a number of edited books, e.g., [41, 42, 43, 44]. CTRW and fractional diffusion emerged to be linked *de facto* under certain mild conditions in 1985 when, without referring to fractional operators, Balakrishnan showed for the first time a similar integral representation [45], but unfortunately without well-posing the problem with respect to the initial condition. The link between CTRW and fractional diffusion was indeed derived on rigorous basis only in 1995 by Hilfer and Anton [46], after that in 1993 the CTRW were linked to fractional relaxation phenomena by Glöckle and Nonnenmacher [47]. So, the correct setting of the CTRW in the framework of non-local fractional operators was derived quite

late in spite of the fact that the relation between the CTRW and the generalised Master equation was already known since the 70s [48, 49, 50, 51], as well as the use of Fourier and Laplace multipliers in the framework of the CTRW [52, 16], and very close results were obtained in the 80s [53, 54, 55, 56]. For a critical review about the link between the CTRW and fractional calculus, the reader is referred to the introductory section in reference [57] and to references [58, 59]. However, the link CTRW–fractional diffusion is only an oversimplified picture that is unable to cover the rich phenomenology that has a place behind the label of anomalous diffusion, but for sure it was the most successful way for the scientific community to become acquainted with anomalous diffusion and to bring out the most important observables.

During the years, anomalous diffusion was slowly established both theoretically, see, e.g., the interpretation of fractional calculus as a macroscopic manifestation of randomness [60] or the relation with Hamiltonian chaos [61], and experimentally, see, e.g., [62, 63, 64, 65, 66], up to the recent confident exhortation by Metzler: "Experimentalists, keep reporting unexpected behaviors!" [67].

In the last decades, a plethora of models were proposed and investigated, each one for fixing and explaining some observables, see, e.g., [68, 69, 70, 71, 72, 73, 74, 75, 76, 77, 78, 79, 80]. Among these recent models, the so-called diffusing-diffusivity (DD) approach [81] resulted to be well performing with respect to some relevant features. The DD approach is based on two stochastic differential equations (SDEs): the over-damped Langevin equation for driving the walker's trajectory and a SDE for the time-dependent diffusion coefficient. This two-equation model resembles the subordination approach and it leads to a superstatistical solution at elapsed time shorter than the correlation time-scale of the diffusion coefficient [81]. In particular, the DD approach allows for a transition from an exponential walker's PDF to a Gaussian PDF displaying also the Brownian yet non-Gaussian (BynG) interval [81, 82].

To conclude this section, in this paper we show, by adopting the CTRW formalism, that anomalous diffusion can emerge from a co-existing pair of well-set Markovian hopping-trap mechanisms with only two different time-scales. Therefore, it is not needed indeed to introduce a broad distribution of relaxation times [1, 2] and neither cumbersome random-walk models. Actually, this model meets many ensemble and also single-particle statistics that define anomalous diffusion: in particular, the transitions of the walker's PDF and the BynG interval like the DD model does. The present model has a number of analogies with the DD-like model recently studied by Hidalgo–Soria, Barkai and Burov [83]. That model is based on an over-damped Langevin equation for a Gaussian process with a dichotomous diffusion coefficient that switches after a random time. The main difference with the present research lays on the fact that any DD-like approach describes through the Langevin equation a pure Lagrangian point-of-view of the continuous walker's wandering by a fully characterisation in terms of the elapsed time. In our CTRW setting, the Eulerian point-of-view of the hopping-trap mechanism is privileged, and the adoption of two Markovian mechanisms allows for fulfilling the Onsager principle [84]. Moreover, recent e-prints appeared [85, 86] where the authors,

motivated by experimental parameters for tau proteins in neuronal cells, through a simple Markovian mobile-immobile transport of particles, which has some similarities with the present model, unveil certain features of anomalous diffusion as the transitions of the walker's PDF by including also the BynG interval.

The rest of the paper is organised as follows. In section 2 we report the features of the paradigmatic anomalous diffusion. In section 3 we introduce the model and in section 4 we present and discuss the results of an intense study by simulations. Conclusions are reported in final section 5.

## 2. The paradigmatic anomalous diffusion

With the advent of techniques for single-particle tracking in living systems, anomalous diffusion found a paradigmatic setting on the basis of experimental data, see, e.g., [71, 87]. Let  $t \geq 0$  be the time-parameter and  $\Omega$  be the sample space, then we denote a stochastic process in unbounded domain by  $X_t^\omega : [0, \infty) \times \Omega \rightarrow \mathbb{R}$  where  $\omega \in \Omega$  indexes each independent realization (namely, each single-particle trajectory). What we call *paradigmatic anomalous diffusion* is a generic one-dimensional random walk diffusing in an unbounded domain that meets the followings features.

At the level of ensemble statistics, anomalous diffusion displays a regime characterized by a MSD that grows in time according to a sub-linear power-law, namely

$$\mathbb{E}[X_t^2] \sim t^\beta, \quad 0 < \beta < 1, \quad (1)$$

and a stretched-exponential distribution that is related to the anomalousness parameter  $\beta$  by

$$\rho(z) \sim |z|^{(\beta-1)/(2-\beta)} \exp\{-|z|^{2/(2-\beta)}\}, \quad |z| \rightarrow +\infty. \quad (2)$$

Here, we refer to (2) as the time-fractional diffusion law.

In terms of FP equation, this phenomenology is modelled by the time-fractional diffusion equation [23, 27, 28], that is the governing equation, for example, of the walker's distribution in the case of the CTRW with infinite-mean waiting times [46] or of the gray Brownian motion (gBm) by Schneider [88, 89]. This last was originally based on the over-damped fractional Brownian motion (fBm) but it could be extended to the under-damped Langevin equation as well [74]. In terms of physical interpretation, the approach based on the CTRW describes a diffusion process in an inhomogeneous medium [90, 91] while the approach based on the gBm describes a diffusion process by an heterogeneous ensemble of walkers [74]. Another stochastic modelling, whose walker's PDF is governed by the time-fractional diffusion equation, is the subordination approach [68] and it is somehow related to the CTRW [92]. In this approach, the Bm evolves with respect to an operational time that is a random variable driven by the physical time. Such randomness can indeed be re-phrased as a randomness of the time-scale of the physical time [93].

At the same time, the anomalous diffusion regime is indeed an intermediate regime, and further features emerged as well as prototypical features of the anomalous

diffusion from the improved experimental capacities [18, 71, 87, 94]. So, nowadays, the paradigmatic anomalous diffusion includes also a walker's distribution  $\rho(x; t)$  with exponential tails at short elapsed time,  $t \ll \tau_B$ , i.e.,  $\rho(z) \sim e^{-|z|}$  as  $|z| \rightarrow +\infty$ , where  $\tau_B$  stays for the Barkai–Burov time-scale who proved that such exponential tails (up to a logarithmic correction:  $\rho(x; t) \sim e^{-|x| \log(|x|/t)^\gamma - Ct}$  as  $|x|/t \rightarrow +\infty$  and  $\gamma, C > 0$ ) are indeed universal for diffusing walkers [95, 96], and also a distribution with Gaussian tails at large elapsed times,  $t \gg \tau_D$ , i.e.,  $\rho(z) \sim e^{-z^2}$  as  $|z| \rightarrow +\infty$ , where  $\tau_D$  stays for the normal diffusion time-scale when, as a matter of fact, walkers go through a Brownian and Gaussian diffusion (anomalous-to-normal transition) [97, 98, 76]. We remark that here the universal exponential-tailed distribution by Barkai & Burov [95] is intended as small-time universality rather than as large-space universality: this exchange is done on the basis of the limit  $|x|/t \rightarrow \infty$ . The ensemble phenomenology is finally enriched by the mentioned BynG interval [81, 82], when the MSD starts to grow linearly in time before than the anomalous-to-normal transition occurs, namely at  $\tau_B \ll \tau_{\text{BnG}} \ll t \ll \tau_D$ . Within these PDF-transitions, the DD approach emerged to be the higher flexible formulation [81, 83]. In its minimal-model scheme, the diffusion coefficient in the DD approach is determined by the square of an Ornstein–Uhlenbeck process and this introduces an extra time-scale that allows for a transition of the walker's PDF through the mentioned regimes and also for the appearing of the BynG interval. The PDF-transition is the strength point of the DD model with respect to other superstatistical-like approaches as: the gBm [88, 89] and the generalized gray Brownian motion (ggBm) [73], which are both superstatistical-like fBm [99], that indeed do not display a transition of the walker's PDF between different shapes. The CTRW approach allows indeed for the anomalous-to-normal transition [100], that can be observed also in the under-damped ggBm as a consequence of the finite statistical sampling of the time-scales [76].

At the level of single-particle statistics, the observables that characterize anomalous diffusion are the p-variation test [101, 102], the time-averaged MSD (TAMSD) and the ensemble-averaged TAMSD (ETAMSD). The p-variation test provides information on the stochastic origins of the data allowing for discriminating among processes. The TAMSD and the ETAMSD allow for observing the dependence of the statistics on the time-lag between the start of the process and the start of the measurement [103, 104, 94], which is called aging. TAMSD and ETAMSD also allow for estimating the degree of ergodicity breaking [105, 106], namely when the walkers need an infinite time for exploring an infinite system but they can access to the whole domain because it is not split in mutually inaccessible regions [105]. In formulae they are as follows.

Let  $T$  be the measurement time, i.e.,  $t \in [0, T]$ , with time-step  $h$  such that  $T = Nh$  and  $\Delta = mh$ , where  $N, m \in \mathbb{N}$  and  $N > m$ , then the p-variation test  $V^{(p)}(t)$  is defined as

$$V^{(p)}(t) = \lim_{n \rightarrow \infty} \sum_{j=0}^{2^n - 1} |X_{t_{j+1} \wedge t} - X_{t_j \wedge t}|^p, \quad \text{with } 2^n = N, \quad (3)$$

where  $t_j = jT/2^n$  and  $a \wedge b = \min\{a, b\}$ . The TAMSD is calculated by the formula

$$\overline{\delta^2}(T, \Delta) = \frac{1}{N - m + 1} \sum_{k=0}^{N-m} [X_{kh+\Delta} - X_{kh}]^2, \quad (4)$$

as a function of  $\Delta$ , while when the ETAMSD  $\mathbb{E}[\overline{\delta^2}]$  is calculated as a function of  $T$  then aging is observed. Finally, the degree of ergodicity breaking is estimated by the parameter

$$E_B(T, \Delta) = \lim_{T \rightarrow \infty} \frac{\mathbb{E}[\overline{\delta^2}]}{\mathbb{E}^2[\overline{\delta^2}]} - 1. \quad (5)$$

Actually,  $E_B$  is an indicator of the inequality between time-averaged and ensemble-averaged statistics.

Paradigmatic anomalous diffusion displays a p-variation consistent with Gaussian processes, in particular with the fBm [101]. Moreover, TAMSD displays a linear growing in time, suggesting an underlying Bm, but the diffusion coefficient differs among single-trajectories, see, e.g., reference [94]. The distribution of the diffusion coefficients among the trajectories causes the weak ergodicity breaking [107, 94, 73]. The CTRW [107], the subordinated fBm [108] and the ggBm [73] have the same degree of ergodicity breaking, i.e., they provide the same value of  $E_B$ . Furthermore, anomalous diffusion in living systems displays aging with an ETAMSD that decreases as  $T^{-\lambda}$  with  $\lambda > 0$  [103, 104, 94]. All these properties are reproduced by the ggBm [73], while the CTRW cannot reproduce the p-variation test [101] together with other failures [94].

### 3. The model

#### 3.1. Definition

We propose a model based on the theory of the CTRW, see references [6, 109, 110, 111, 112] for technical and historical reviews. Let  $\Omega$  be the sample space, then  $\omega \in \Omega$  indexes each independent realization of the walker's trajectory. In the CTRW approach, each  $\omega$ -realization of the walker's trajectory goes through the pair of iterative processes

$$X_N^\omega - X_{N-1}^\omega = R_N, \quad t_N^\omega - t_{N-1}^\omega = \tau_N, \quad N = 1, 2, \dots, \quad (6)$$

where the displacements  $R$  are i.i.d. random variables distributed according to the jump-size distribution  $\lambda(x)$  and the positive time-increments  $\tau$  between consecutive jumps are i.i.d. random variables distributed according to the waiting-time distribution  $\psi(t)$  such that, after  $N$  iterations, the walker of the  $\omega$ -realization is located in  $X_N^\omega = x_0 + \sum_{i=1}^N R_i$  at the elapsed time  $t_N^\omega = t_0 + \sum_{i=1}^N \tau_i$ . It holds that, for the same number of iterations  $N$ , the elapsed times of two different  $\omega$ -realizations are different. We can compress this notation in  $(X_N^\omega, t_N^\omega) = X_{t_N^\omega}^\omega$ . We set  $x_0 = 0$  and  $t_0 = 0$ .

Without loss in generality, we consider the case of a random walk in continuous space, rather than in a lattice, and then  $X_{t_N^\omega}^\omega : [0, +\infty) \times \Omega \rightarrow \mathbb{R}$  with  $\lambda(x) : \mathbb{R} \rightarrow \mathbb{R}_+$

and  $\psi(t) : \mathbb{R}_+ \rightarrow \mathbb{R}_+$ . Within the formalism of the uncoupled CTRW [113], if  $\rho(x; t) : \mathbb{R} \times (0, +\infty) \rightarrow \mathbb{R}_+$  is the walker's PDF at site  $x \in \mathbb{R}$  and time  $t > 0$  with initial datum  $\rho(x; 0) = \delta(x)$ , such that  $\int_{\mathbb{R}} \rho(x; t) dx = 1$  and  $\rho(x; t) > 0$  for all  $(x, t) \in \mathbb{R} \times (0, +\infty)$ , then in the Fourier–Laplace domain it holds

$$\widehat{\rho}(\kappa; s) = \int_0^{+\infty} e^{-st} \int_{-\infty}^{+\infty} e^{-i\kappa x} \rho(x; t) dx dt = \frac{1 - \widetilde{\psi}(s)}{s[1 - \widehat{\lambda}(\kappa)\widetilde{\psi}(s)]}, \quad (7)$$

where  $\widetilde{\psi}(s)$  and  $\widehat{\lambda}(\kappa)$  are the Laplace and the Fourier transforms of the waiting-time distribution  $\psi(t)$  and of the jump-length distribution  $\lambda(x)$ , respectively. Since from the normalization condition of  $\psi(t)$  and  $\lambda(x)$  it follows that  $\widetilde{\psi}(0) = \widehat{\lambda}(0) = 1$ , then it holds  $\widehat{\rho}(0; s) = 1/s$ .

The memory of the process is provided by the waiting-time distribution  $\psi(t)$ . In fact, by inverting (7) we have that the FP equation is [32]

$$\int_0^t \Phi(t - \tau) \frac{\partial \rho}{\partial \tau} d\tau = -\rho(x; t) + \int_{-\infty}^{+\infty} \lambda(x - \xi) \rho(\xi; t) d\xi, \quad (8)$$

where the memory kernel  $\Phi(t)$  is defined by

$$\widetilde{\Phi}(s) = \frac{1 - \widetilde{\psi}(s)}{s\widetilde{\psi}(s)}. \quad (9)$$

Therefore, the process is memory-less, i.e., Markovian, when  $\Phi(t) = \delta(t/\tau_M) = \tau_M \delta(t)$ , where  $\tau_M$  is the time-scale of the Markovian process, which means  $\widetilde{\Phi}(s) = \tau_M$  and then  $\psi(t) = e^{-t/\tau_M}/\tau_M$  [55, 32] such that the mean waiting-time is:  $\langle t \rangle = \int_0^{+\infty} t \psi(t) dt = \tau_M$ .

We consider a Gaussian jump-length distribution, i.e.,

$$\lambda(x) = \frac{e^{-x^2/(2\sigma^2)}}{\sqrt{2\pi\sigma^2}}, \quad \langle x^2 \rangle = \int_{-\infty}^{+\infty} x^2 \frac{e^{-x^2/(2\sigma^2)}}{\sqrt{2\pi\sigma^2}} dx = \sigma^2, \quad (10)$$

and the following model for the waiting-time distribution

$$\psi(t) = p \frac{e^{-t/\tau_D}}{\tau_D} + (1 - p) \frac{e^{-t/\tau_B}}{\tau_B}, \quad \tau_B \leq \tau_D, \quad (11)$$

where  $p \in [0, 1]$  is the probability of occurrence of each family of Markovian mechanisms:  $\psi_D(t) = e^{-t/\tau_D}/\tau_D$  and  $\psi_B(t) = e^{-t/\tau_B}/\tau_B$ ,  $\tau_D$  is the time-scale of the diffusion-limit and  $\tau_B$  is the Barkai–Burov time-scale [95, 96], both have been discussed in section 2, and the diffusion coefficient results to be  $\mathcal{D} = \sigma^2/(2\langle t \rangle)$  with  $\langle t \rangle = p\tau_D + (1 - p)\tau_B$ .

### 3.2. Non-Markovianity

By using the Laplace transform of the memory kernel (9), we can study the non-Markovianity of model (11). Actually, we obtain

$$\widetilde{\Phi}(s) = \frac{\tau_B(1 + \tau_D s) + p(\tau_D - \tau_B)}{p(1 + \tau_B s) + (1 - p)(1 + \tau_D s)}, \quad (12)$$

and it can be checked that model (11) is Markovian when  $\tau_B = \tau_D = \tau_M$ , such that  $\widetilde{\Phi}(s) = \tau_M$  for all  $p$ , and when  $p = 0$ , such that  $\widetilde{\Phi}(s) = \tau_B = \tau_M$  for arbitrary  $\tau_D$ . At

large time, the memory fades away and then, when  $\tau_D \gg \tau_B$ , we have that in the Laplace domain the large-time limit corresponds to the limit  $s \ll 1/\tau_D \ll 1/\tau_B$  and it holds

$$\tilde{\Phi}(s) \simeq p \tau_D + (1-p) \tau_B = \tau_M, \quad \tau_B s \ll \tau_D s \ll 1, \quad (13)$$

that is an estimation of  $\tau_M$  because in this limit  $\tilde{\Phi}(s)$  is independent of  $s$ . Therefore we have that

$$\tau_M = \tau_B \left( 1 - p + p \frac{\tau_D}{\tau_B} \right), \quad (14)$$

and by assuming that  $\tau_M$  exists and is bounded for all  $p$  and whatever is the inequality  $\tau_D \gg \tau_B$ , it means that  $p \tau_D/\tau_B$  is always bounded for all  $p$  and whatever is the inequality  $\tau_D \gg \tau_B$ , too, such that  $\tau_B \simeq p \tau_D$  when  $p \rightarrow 0$ . In fact, if  $\tau_D < \infty$  then the quantity  $p \tau_D/\tau_B$  is not bounded for all  $p$  when for example  $\tau_B \propto p^2$  and  $p \rightarrow 0$ . To conclude, if we plug  $\tau_B \propto p \tau_D$  into (14), together with  $p \rightarrow 0$  such that  $\tau_D \gg \tau_B$ , we have that  $\tau_M \simeq \tau_B (2-p) \propto 2p \tau_D$  and, by plugging this last into (13), we finally have the following constraints for non-Markovianity

$$\tau_B = \tau_D \frac{p}{1-p}, \quad p \in (0, 1/2), \quad (15)$$

when  $p = 1/2$  then  $\tau_B = \tau_D$  and, according to (12), model (11) results to be Markovian. In particular, constraint (15) provides an estimation of the Barkai–Burov time-scale  $\tau_B$  for defining the small elapsed-times, i.e.,  $t \ll \tau_B$ , and states the time-scale  $\tau_D$  for defining the large elapsed-times, i.e.,  $t \gg \tau_D$ .

Hence, from (9) we have that model (11, 15) is non-Markovian, in fact it holds

$$\tilde{\Phi}(s) = \tau_D \frac{p(1 + \tau_B s) + p(1 + \tau_D s)}{p(1 + \tau_B s) + (1-p)(1 + \tau_D s)}, \quad p \in (0, 1/2), \quad (16)$$

that is dependent on  $s$  when  $\tau_D s \gg \tau_B s \gg 1$  and  $p \in (0, 1/2)$ , and it goes to  $\tilde{\Phi}(s) = 2p \tau_D = \tau_M$  when  $\tau_B s \ll \tau_D s \ll 1$ . Note that in (15) and (16)  $p \neq 0$ , see also below (12), otherwise for model (11, 15) it holds  $\tau_B = 0$  for  $\tau_D < \infty$  and  $\tilde{\Phi}(s) = 0$  for all  $s$ , namely  $\psi(t) = 0$  for all  $t$ .

Moreover, in opposition to literature on CTRW models for anomalous diffusion, see, among many, the reviews [10, 11, 110], the mean waiting-time of model (11, 15) is finite, i.e.,

$$\langle t \rangle = \int_0^{+\infty} t \psi(t) dt = 2p \tau_D = \tau_M < \infty. \quad (17)$$

By setting  $\tau_D < +\infty$ , a finite-mean waiting-times exists (17) which guarantees a transition to normal diffusion.

### 3.3. Power-law memory fading and anomalousness parameter $\beta$

Together with non-Markovianity, model (11) displays also a power-law memory fading. We introduce the so-called survival probability, see, e.g., [109], namely the probability for the walker to remain at the initial position:

$$\Psi(t) = 1 - \int_0^t \psi(\xi) d\xi, \quad \frac{d\Psi}{dt} = -\psi(t), \quad \tilde{\Psi}(s) = \frac{1 - \tilde{\psi}(s)}{s}, \quad (18)$$

that, for the present model (11), is

$$\Psi(t) = p e^{-t/\tau_D} + (1-p) e^{-t/\tau_B}, \quad \tilde{\Psi}(s) = \frac{p \tau_D}{1 + \tau_D s} + \frac{(1-p) \tau_B}{1 + \tau_B s}. \quad (19)$$

It is known that anomalous diffusion is obtained within the CTRW formalism when  $\tilde{\psi}(s) \sim 1 - s^\beta$  with  $s \rightarrow 0$ , e.g., [10], and it is embodied in the CTRW/fractional diffusion formalism by [46]

$$\Psi_{\text{ML}}(t) = E_\beta(-t^\beta), \quad \tilde{\Psi}_{\text{ML}}(s) = \frac{s^{\beta-1}}{s^\beta + 1}, \quad (20)$$

with

$$\tilde{\Psi}_{\text{ML}}(s) \sim \frac{1}{s^{1-\beta}}, \quad s \rightarrow 0, \quad (21)$$

where  $E_\beta(-t^\beta)$ , with  $0 < \beta < 1$ , is the Mittag-Leffler function [114, Appendix E]

$$E_\alpha(z) = \sum_{n=0}^{\infty} \frac{z^n}{\Gamma(1 + \alpha n)}, \quad \alpha > 0, \quad z \in \mathbb{C}. \quad (22)$$

The Laplace transforms of the two survival probabilities (19) and (20) are related by the formula [114, formula (E.51)]

$$\frac{1}{1-s} = \int_0^\infty e^{-u} E_\alpha(u^\alpha s) du, \quad \alpha > 0, \quad (23)$$

and then

$$\begin{aligned} \tilde{\Psi}(s) = p \tau_D \int_0^\infty e^{-u} E_\alpha(-u^\alpha \tau_D s) du \\ + (1-p) \tau_B \int_0^\infty e^{-u} E_\alpha(-u^\alpha \tau_B s) du. \end{aligned} \quad (24)$$

If we consider the interval  $1/\tau_D \ll s \ll 1/\tau_B$  then it holds  $\tau_D s \gg 1$  and  $\tau_B s \ll 1$  such that  $u^\alpha \tau_D s \rightarrow 0$  for  $u \leq u_m(s) \ll (\tau_D s)^{-1/\alpha}$  and  $u^\alpha \tau_B s \rightarrow 0$  for all  $u$ . Therefore, by noting that  $E_\alpha(0) = 1$ , in the interval  $1/\tau_D \ll s \ll 1/\tau_B$ , formula (24) becomes

$$\tilde{\Psi}(s) \simeq \tau_M - p \tau_D e^{-u_m(s)} + p \tau_D \int_{u_m(s)}^\infty e^{-u} E_\alpha(-u^\alpha \tau_D s) du, \quad (25)$$

where definition (13) of  $\tau_M$  has been used. Through the change of variable  $\xi = (\tau_D s)^{1/\alpha} u$ , we have that

$$\tilde{\Psi}(s) \simeq \tau_M - p \tau_D e^{-u_m(s)} + \frac{p \tau_D}{(\tau_D s)^{1/\alpha}} \int_{\xi_m}^\infty e^{-\xi/(\tau_D s)^{1/\alpha}} E_\alpha(-\xi^\alpha) d\xi, \quad (26)$$

where  $\xi_m = (\tau_D s)^{1/\alpha} u_m(s)$  is independent of  $s$ . By looking at the integral term and by remembering that  $\tau_D s \gg 1$ , we observe that for an arranged interval of  $s$  such that  $\xi_m \sim \mathcal{O}(1)$  we finally obtain the following power-law scaling

$$\tilde{\Psi}(s) \simeq \tau_M + \frac{p \tau_D^{1-1/\alpha}}{s^{1/\alpha}} \int_{\xi_m}^\infty E_\alpha(-\xi^\alpha) d\xi, \quad \frac{1}{\tau_D} \ll s \ll \frac{1}{\tau_B}, \quad \alpha > 0. \quad (27)$$

From this derivation the value of  $\alpha$  is indetermined, as a consequence of the indetermination of  $\alpha$  in formula (23). However, the value of  $\alpha$  is expected to be

determined as function of  $p$ , i.e.,  $\alpha = \alpha(p)$ . Moreover, since we are focused on the resulting anomalous diffusion, we can establish a relation between the value of  $\alpha$ , which corresponds to the model (11, 15), and the exponent  $\beta$  as follows from the anomalous diffusion displayed by a CTRW model equipped with (20). Hence, by comparing (27) and (21), we have the relation

$$\beta = 1 - \frac{1}{\alpha(p)}, \quad (28)$$

and we can fix  $\alpha(p)$  by comparing plots of the power-law interval of (19) for different values of  $p$  against plots of (20) for different values of  $\beta$ .

In particular, by writing  $\tilde{\Psi}_{\text{ML}}(s)$  in dimensional form:

$$\tilde{\Psi}_{\text{ML}}(s) = \tau_1 \frac{(\tau_2 s)^{\beta-1}}{(\tau_2 s)^\beta + 1}, \quad (29)$$

and by searching for the time-scales  $\tau_1$  and  $\tau_2$  by comparing (29) against (19), in the limit  $\tau_{\text{B}}/\tau_{\text{D}} \rightarrow 0$  we get

$$\tilde{\Psi}_{\text{ML}}(s) \simeq \tilde{\Psi}(s), \quad s \gg \frac{1}{\tau_2}, \quad \text{with} \quad \tau_1 = p \tau_{\text{D}}, \quad \tau_2 = 2 \frac{\tau_{\text{D}} \tau_{\text{B}}}{\tau_{\text{D}} + \tau_{\text{B}}}. \quad (30)$$

The Laplace transforms of the two survival probabilities, i.e.,  $\tilde{\Psi}_{\text{ML}}(s)$  in (20) and  $\tilde{\Psi}(s)$  in (19), are compared in figures 1 and 2.

In figure 1 we observe that the two survival probabilities display an universal behaviour for large values of  $s$  with respect to the associated short-time time-scales: this corresponds to the universal behaviour for short elapsed-times related to the Barkai–Burov time-scale  $\tau_{\text{B}}$ , i.e.,  $s \gg 1/\tau_{\text{B}}$ .

In figure 2 we observe that, for small enough  $p$ , the two survival probabilities display a parallel power-law decreasing for intermediate values of  $s$  for a couple of decades around the large-time time-scale  $\tau_{\text{D}}$ . At very large-time, i.e.,  $s \ll 1/\tau_{\text{D}}$ , the present model transits to the normal diffusion while the CTRW equipped with the survival probability  $\Psi_{\text{ML}}(t)$  continues with the anomalous diffusion.

Moreover, searching for the common power-law between  $\tilde{\Psi}_{\text{ML}}(s)$  and  $\tilde{\Psi}(s)$  in the interval around  $\tau_{\text{D}}s = 1$  leads to a determination of the anomalousness parameter  $\beta$ , see figure 3, that emerges to be approximated by the formula

$$\beta \simeq 1 - \frac{1}{1 + \log \frac{1-p}{p}}, \quad p \in (0, 1/2), \quad (31)$$

and then we have from (28) that

$$\alpha(p) = 1 + \log \frac{1-p}{p}, \quad p \in (0, 1/2). \quad (32)$$

Again we have that  $p \neq 0$ , otherwise  $\beta = 1$  and anomalous diffusion is lost. On the contrary, we have that when  $p = 1/2$  it holds  $\beta = 0$  such that diffusion stops as an extreme consequence of sub-diffusion. However, when  $p = 1/2$  the model (11, 15) reduces to Markovian standard diffusion and anomalous diffusion is lost again. An

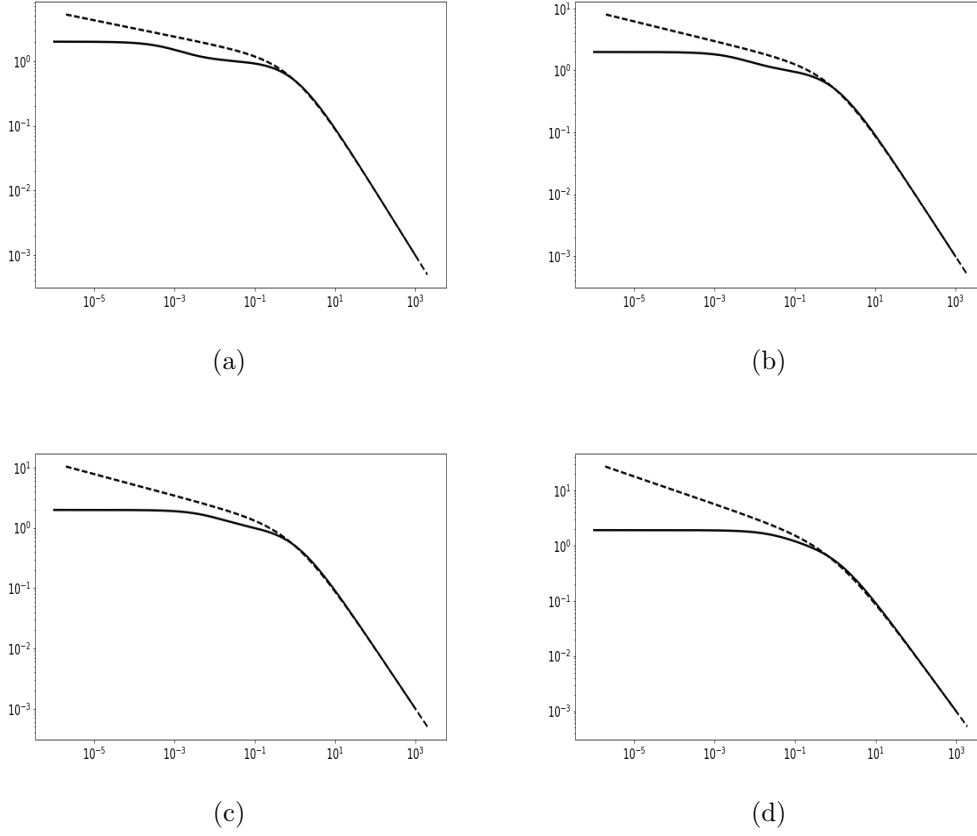


Figure 1: Plots of the Laplace transforms of the survival probabilities  $\tilde{\Psi}_{\text{ML}}(s)/\tau_1$  vs  $\tau_2 s$  (dashed line) and  $\tilde{\Psi}(s)/\tau_B$  vs  $\tau_B s$  (continuous line) for different values of  $p \in (0, 1/2)$ , from (a) to (d):  $p = 0.001, 0.005, 0.01, 0.05$ . The universal short-time behaviour is evident by the overlapping of the two curves for large values of the corresponding arguments and starting at  $\tau_2 s = 1$  and at  $\tau_B s = 1$ , respectively.

explanation follows from the estimation of the extension of the anomalous diffusion interval by the difference

$$\tau_D - \tau_B = \tau_D \left( 1 - \frac{p}{1-p} \right), \quad (33)$$

where (15) has been used. From formula (31) we finally obtain that the extension of the anomalous diffusion interval is

$$\tau_D - \tau_B = \tau_D \left[ 1 - e^{-\beta/(1-\beta)} \right], \quad (34)$$

that decreases when  $\beta$  decreases and we have the ratio

$$\frac{\tau_B}{\tau_D} = e^{-\beta/(1-\beta)}. \quad (35)$$

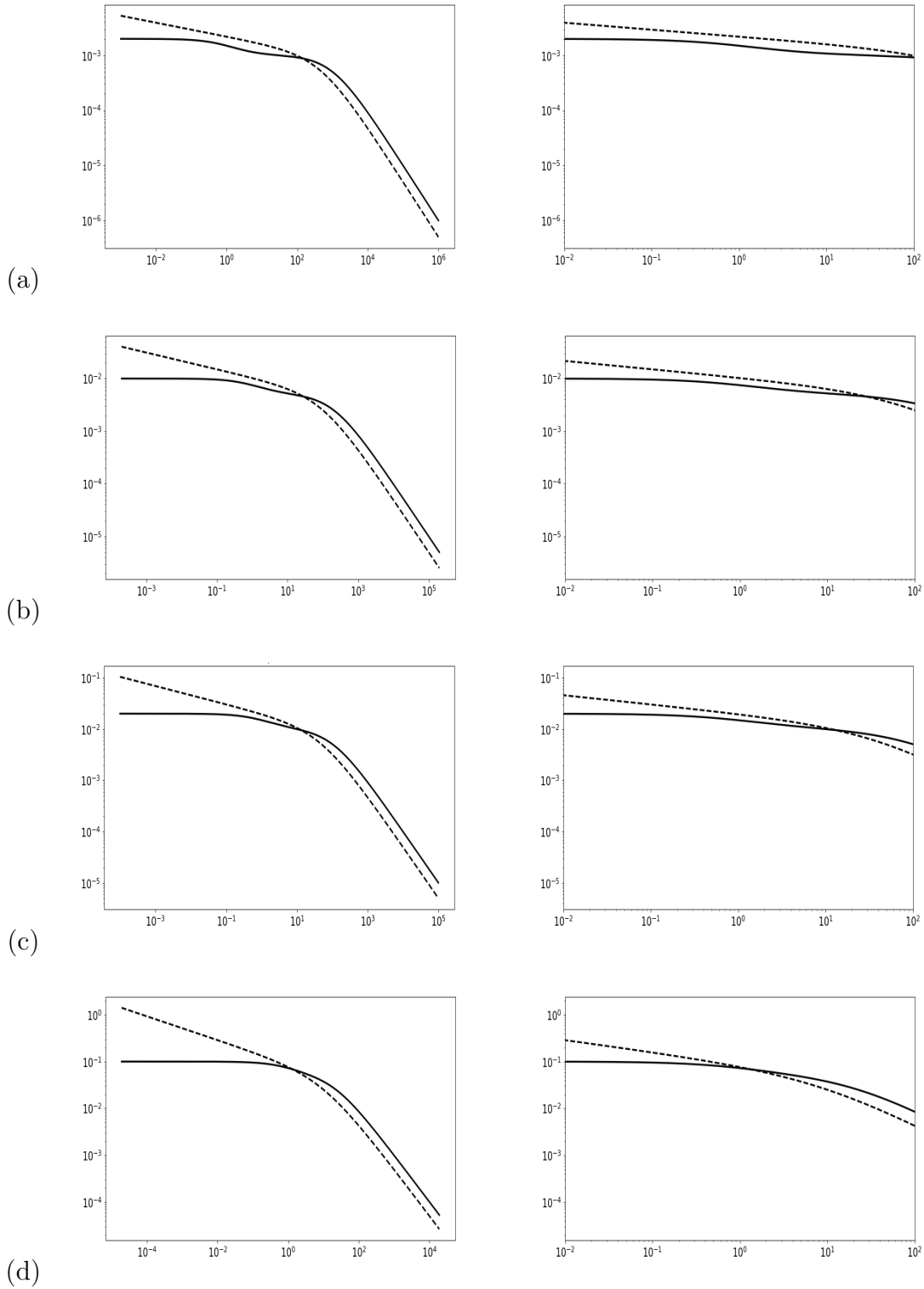


Figure 2: Plots (left column) of the Laplace transforms of the survival probabilities  $\tilde{\Psi}_{\text{ML}}(s)/\tau_{\text{D}}$  vs  $\tau_{\text{D}}s$  (dashed line) and  $\tilde{\Psi}(s)/\tau_{\text{D}}$  vs  $\tau_{\text{D}}s$  (continuous line) for different values of  $p \in (0, 1/2)$ , from (a) to (d):  $p = 0.001, 0.005, 0.01, 0.05$ . It is evident that for small enough  $p$  there exists an intermediate interval of a couple of decades located around  $\tau_{\text{D}}s = 1$  where both Laplace transforms of the survival probabilities display a power-law decaying, see the zoom in the right column.

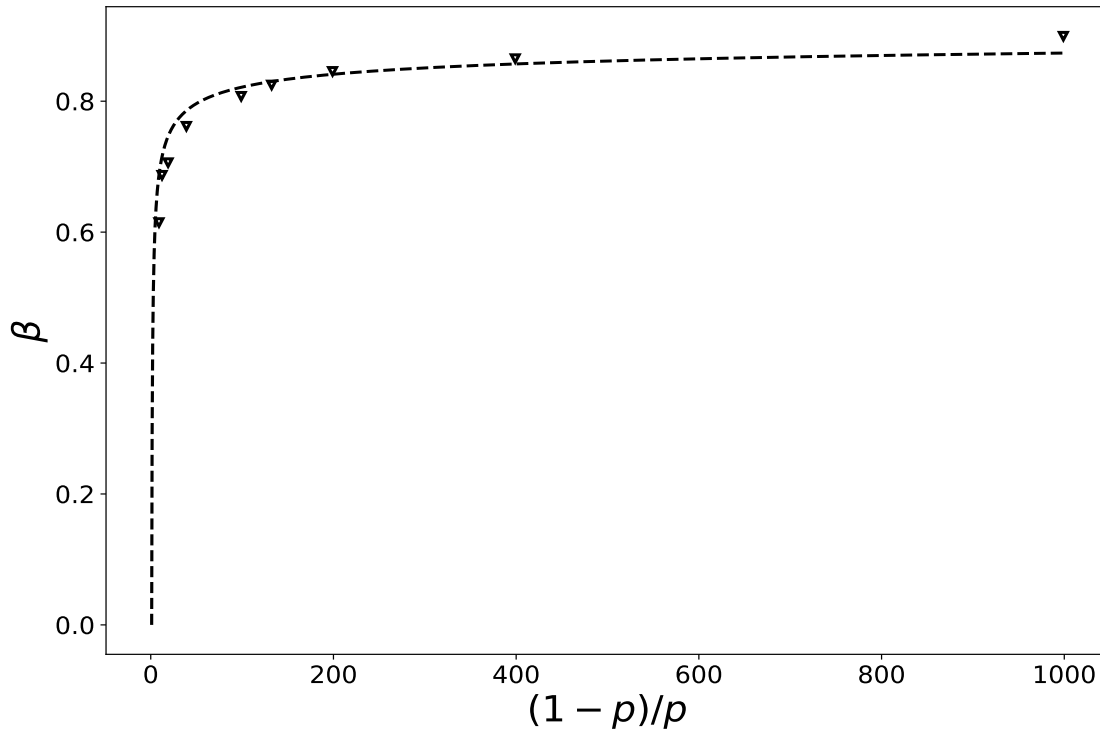


Figure 3: Determination of the anomalousness parameter  $\beta$  by plotting the parameter  $\beta$  of  $\tilde{\Psi}_{\text{ML}}(s)$  and the ratio  $(1-p)/p$  of  $\tilde{\Psi}(s)$  as they emerge in the equal power-law decaying interval in figure 2. The fit is given in formula (31).

### 3.4. Further to model (11, 15)

Present model (11, 15) is fully determined by a pair of dimensional parameters, i.e.,  $[\tau_{\text{B}}] = \text{Time}$  and  $[\sigma] = \text{Length}$ , and one single adimensional parameter, i.e.,  $p \in (0, 1/2)$ . When  $p = 1/2$  the model reduces to the Markovian normal diffusion with  $\tau_{\text{D}} = \tau_{\text{B}} = \tau_{\text{M}}$  and  $\tilde{\Phi}(s) = \tau_{\text{M}}$  such that the mean waiting-time is  $\langle t \rangle = \tau_{\text{M}}$ .

We highlight that the present model (11) is not a two-state CTRW [115]. It is indeed much more close to the model studied by Hilfer in his objection to the relation between the CTRW and time-fractional diffusion equations [58] and to the models studied by Barkai and Sokolov in their subsequent reply [59]. Those models [58, 59] were based on a waiting-times distribution built by the combination of a power-law and an exponential-law: a recent analog study showed that for an inhomogeneous version of that model a weak form of the objection still holds [116] because normal diffusion can be observed for a particular interval of the exponent of the power-law. Similarly, model (11) relates also with the double-order time-fractional diffusion equation in the Caputo sense [117, 118, 119] by plugging into (8) the memory kernel  $\Phi(t)$  as defined in (9) and split according to (11). Furthermore, model (11, 15) shares with the Weistrass random-walk for Lévy flights [120, 121] the fact that it allows for the estimation of the anomalousness parameter from the dynamics of the process, and it is not indeed plugged

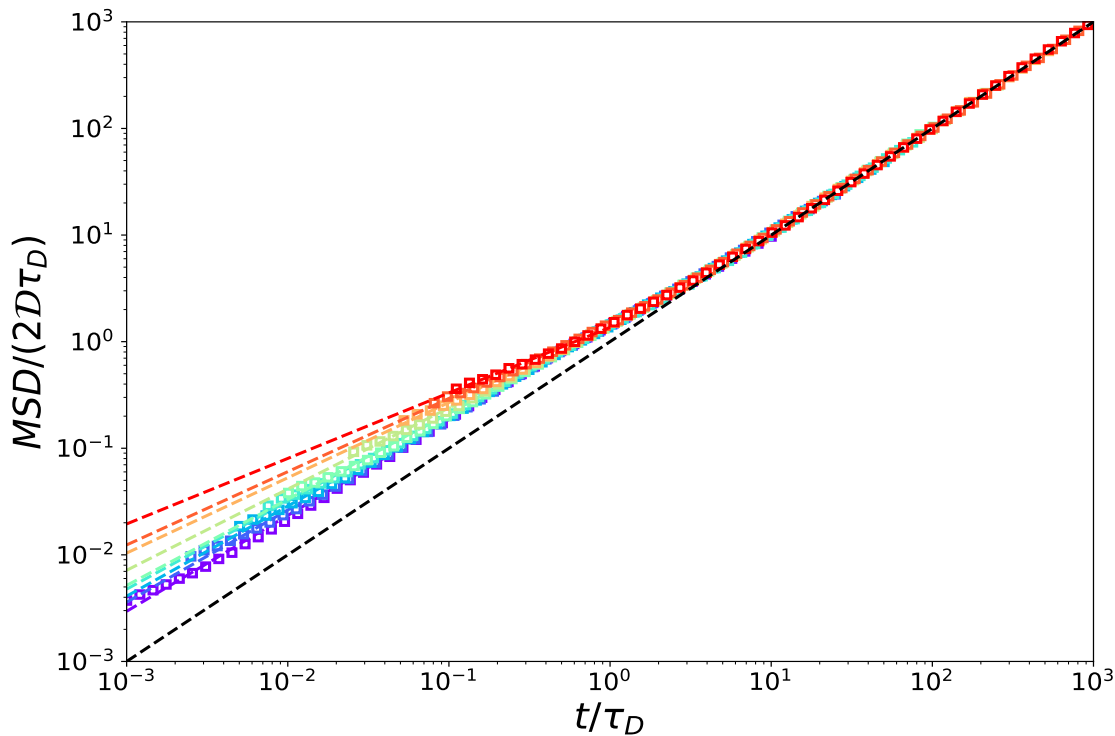


Figure 4: Plots of MSD for different values of  $p \in (0, 1/2)$ . The plots show that at large-times  $t > \tau_D$  the model (11, 15) diffuses according to standard diffusion while at intermediate-times  $\tau_B < t < \tau_D$  diffuses anomalously with parameter  $\beta$  dependent on  $p \in (0, 1/2)$ . The values of  $p$  adopted for this figure are  $p = 0.001, 0.0025, 0.005, 0.0075, 0.01, 0.025, 0.05, 0.075, 0.1$ . Coloured dashed-lines correspond to the estimation of the anomalousness parameter  $\beta$  as plotted in figure 3 and fitted by formula (31).

into the formulation.

Beside all of this, we have that two families of Markovian mechanisms are enough for generating an anomalous diffusive regime, in opposition to the Mittag-Leffler formalism that claims for a large spectrum of families of Markovian mechanisms [2]. Moreover, much more unbalanced is the occurrence of each family of Markovian mechanisms, i.e.,  $p \rightarrow 0^+$ , much more solid is the intermediate interval where anomalous diffusion is generated by a power-law memory fading. Actually, the approximation of power-law functions through exponential sums has been already investigated [122, 123, 124]. Theoretically, this is the main result of the present paper and, with respect to the existing literature, we want to stress that the present model (11, 15) liberates research on anomalous diffusion from the shackles of power-law or infinite mean.

In the following we show through intensive simulations that this two Markovian hopping-trap mechanisms are enough for obtaining a random walk that meets the features that define the here-called paradigmatic anomalous diffusion.

#### 4. Simulations

In spite of its simple definition, we computed no further analytical result, yet, and we present here an intensive study based on simulations. Model (11, 15) is investigated with respect to its regime-transitions with focus on the intermediate regime. Such intermediate regime can be long enough to characterize the process. A similar study on Lévy flights showed that, in some special settings, an intermediate regime could extend so much to making the large-time limit unattainable from measurements in real systems [125].

The setting of simulations is the following: the number of independent realizations is  $\max\{\omega \in \Omega\} = 10^4$ , the two dimensional parameters are  $\tau_B = 1$  and  $\sigma = 1$ , and different values of  $p \in (0, 1/2)$ .

We report the outputs of model (11, 15) regarding the observables proper of the paradigmatic anomalous diffusion presented in section 2. We start this numerical study with ensemble statistics. The MSD is shown in figure 4 and we observe that the MSD displays an anomalous sub-linear regime with exponent  $\beta$  when  $\tau_B < t < \tau_D$  and Brownian linear diffusion when  $t > \tau_D$ . For different values of  $p$  different values of  $\beta$  follow according to formula (31). Furthermore, consistently with the paradigmatic anomalous diffusion discussed in section 2, the walker's PDF of model (11, 15) goes through regime-transitions. In particular, in figure 5 it is shown that when the walker's PDF is re-scaled with the corresponding variance, we can distinguish three different tail-behaviours: exponential ( $t < \tau_B$ ), stretched-exponential ( $\tau_B < t < \tau_D$ ) and Gaussian ( $t > \tau_D$ ). In particular, we can see that the stretched-exponential PDF follows the time-fractional diffusion law (2) and the anomalousness parameter  $\beta$  is dependent on  $p$  according to formula (31). Moreover, we observe that when  $p = 1/2$  the walker's PDF transits from the exponential to the Gaussian by skipping the stretched-exponential, that is in agreement with the Barkai–Burov theory [95]. This is consistent also with the previous analysis where, from formula (31), we have that  $\beta = 0$  when  $p = 1/2$  and then the duration of the anomalous diffusion interval is  $\tau_D - \tau_B = 0$  according to formula (34).

We end the analysis of the ensemble statistics by discussing the occurrence of the BynG interval. In particular we plot in the same figures the MSD and the kurtosis to compare the starting of the Brownian linear scaling of the MSD against the Gaussianity of the PDF, this last is expressed through its kurtosis value  $K = 3$ . First of all we observe that the hopping-trap mechanism intrinsically displays a delay in the spirit of the BynG with respect to continuous processes. This is shown in figure 6 where the basic Markovian CTRW model ( $p = 1/2$ ) displays a one-decade of delay while this delay is indeed not displayed at all by the over-damped Langevin equation, i.e.,  $dY_t^\omega = \sqrt{2D} dW_t^\omega$ , with  $\omega \in \Omega$ , where  $Y_t^\omega : [0, +\infty) \times \Omega \rightarrow \mathbb{R}$  and  $dW_t^\omega$  is the delta-correlated Wiener process with variance  $\mathbb{E}[(dW_t)^\omega]^2 = dt$ .

The BynG interval for model (11, 15) is shown in figure (7). Qualitatively, we observe that the kurtosis has an oscillating behaviour, as a consequence of the action

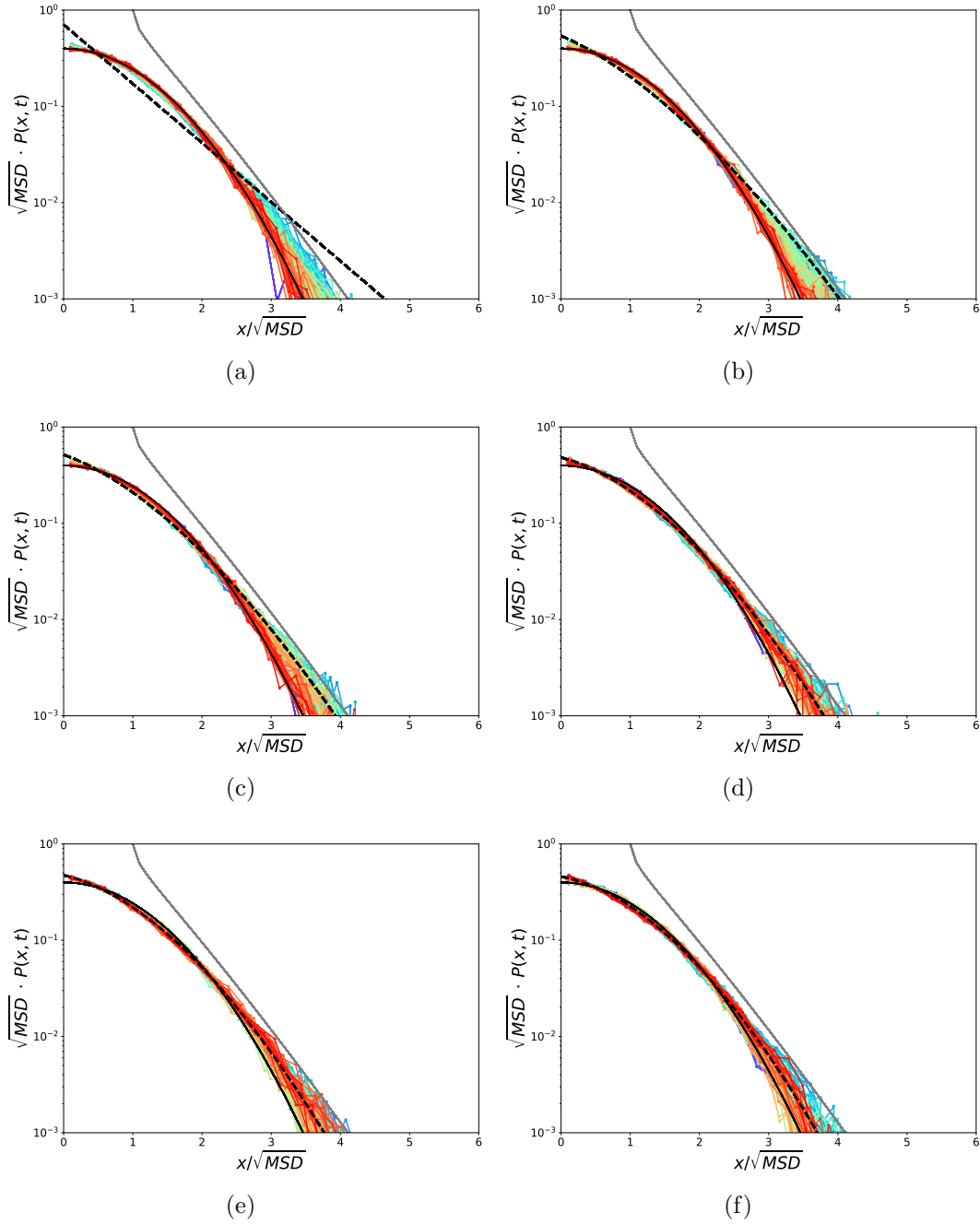


Figure 5: Plots of walker's PDF at different elapsed-times for different values of  $p \in (0, 1/2]$ , from (a) to (f):  $p = 0.5, 0.1, 0.05, 0.01, 0.005, 0.001$  that is  $\beta = 0, 0.6872, 0.7465, 0.8213, 0.8411, 0.8735$ . The PDF goes through two regime-transitions from short-time  $t < \tau_B$  (violet), to intermediate-time  $\tau_B < t < \tau_D$  (green), and to large-time  $t > \tau_D$  (red). The reference lines for PDF tails corresponds to the exponential (gray solid-line), to the stretched-exponential (black dashed-line), and to the Gaussian (black solid-line). The stretched-exponential PDF follows the time-fractional diffusion law (2). It is important to observe that when  $p = 0.5$  the tails of the PDF transit from exponential to Gaussian by skipping the stretched-exponential that is in agreement with the Barkai–Burov theory [95].

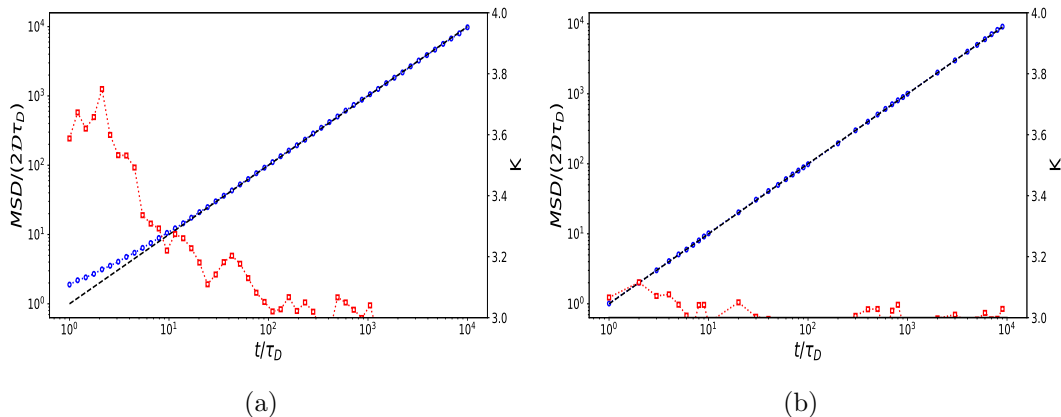


Figure 6: Comparison of the starting of the Brownian linear scaling of the MSD (blue) against the kurtosis (red), this last expresses through its value  $K = 3$  the Gaussianity of the PDF. In panel (a) it is reported the behaviour of the basic Markovian CTRW ( $p = 1/2$ ) and in panel (b) that of the over-damped Langevin equation. An intrinsic BynG delay of one decade is displayed by an hopping-trap mechanism with respect to a continuous stochastic process.

of two co-existing Markovian mechanisms acting on the walker with different statistical frequency (11). Quantitatively, we observe that the intrinsic one-decade delay of an hopping-trap mechanism, see panel (a) of both figures 6 and 7, increases for decreasing values of  $p$  up to an extension of two decades of the relaxation time for the diffusive limit  $\tau_D$ . This behaviour can be compared against the behaviour of the minimal DD model displayed in [81, figure 3]. In particular, the duration of the BynG interval in the minimal DD model is two decades with respect to the relaxation time of the stochastic diffusion coefficient. Therefore, the BynG interval of the present model (11, 15) is comparable with that of the prototypical DD model [81].

About statistics of single-trajectory, in figure 8 it is shown that model (11, 15) displays a p-variantion test consistent with an underlying Gaussian-like motion, e.g., the fBm [101] and ggBm [73], and then consistent also with the typical signature of motion inside living cells, see, e.g., [101]. Moreover, in figure 9 it is shown that the TAMSD scales linearly as the Bm but it displays a distribution of diffusion coefficients among the trajectories. This behaviour is also observed in data of molecular motion in living cells, see, e.g., [94]. Together with the p-variation trend, the TAMSD is another characteristic consistent with the ggBm formalism [126, 73] that, for a distribution of the diffusion coefficients which is characteristic of each data set, was successfully applied to anomalous diffusion observed in live *Escherichia coli* bacteria by tracking mRNA molecules, see reference [64] for the data and [99] for the ggBm-like model, and by tracking DNA-binding proteins, see reference [127] for the data and [79] for the ggBm-like model. The distribution of the diffusion coefficient causes weak ergodicity-breaking

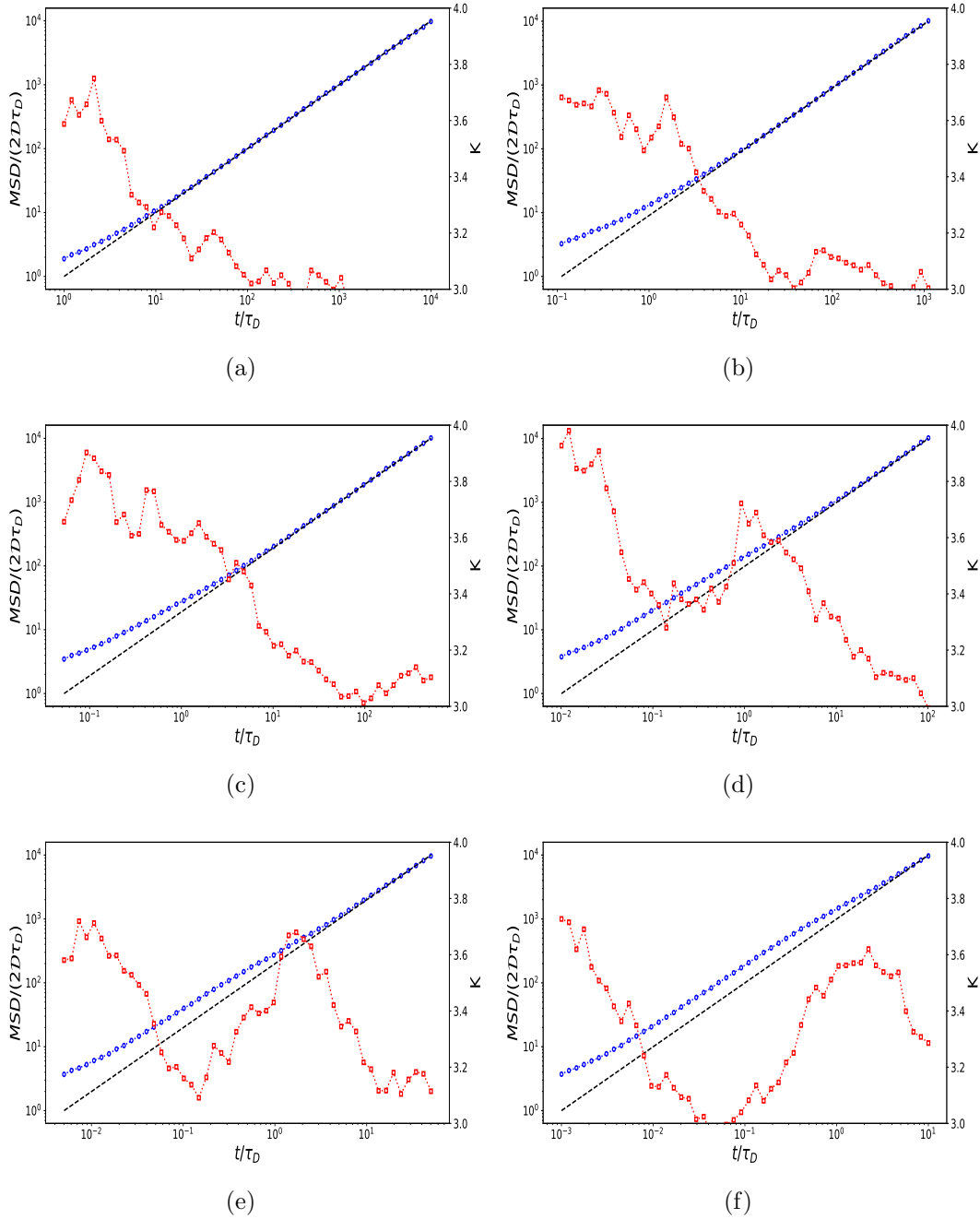


Figure 7: The same as in figure 6 for model (11, 15) only with different values of  $p \in (0, 1/2]$ , from (a) to (f):  $p = 0.5, 0.1, 0.05, 0.01, 0.005, 0.001$ . Panel (a) shows the basic Markovian CTRW model ( $p = 1/2$ ) as in panel (a) of figure 6, it is shown again for convenience for comparison with model (11, 15). The oscillating behaviour of the kurtosis reflects the action of two co-existing Markovian mechanisms acting on the walker with different statistical frequency (11). The intrinsic one-decade delay of an hopping-trap mechanism displayed in panel (a) increases for decreasing values of  $p$  up to an extension of two decades.

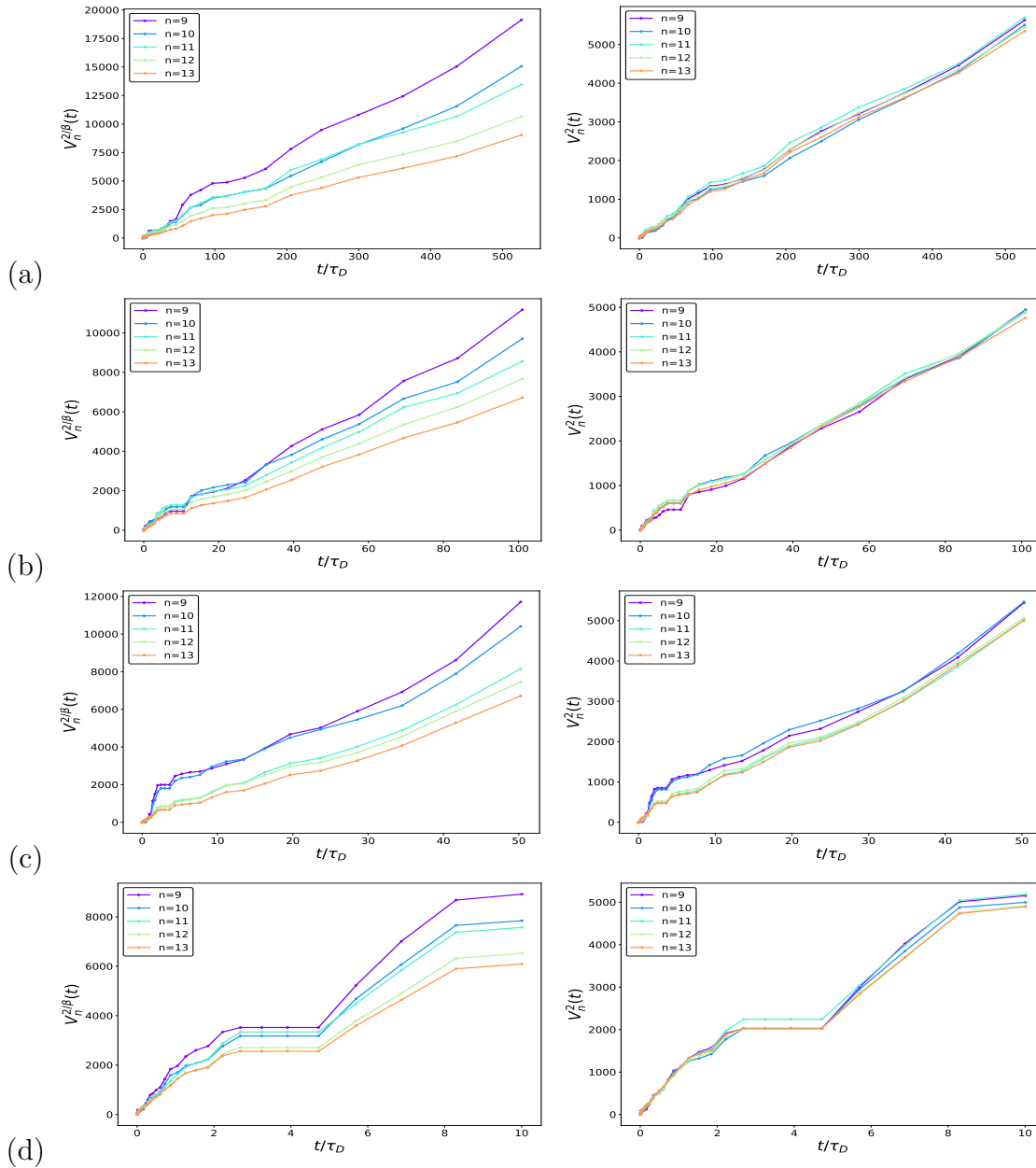


Figure 8: Plots of  $p$ -variation tests of variation orders  $2/\beta$  (left) and 2 (right) for different values of  $p \in (0, 1/2)$ , from (a) to (d):  $p = 0.05, 0.01, 0.005, 0.001$  that is  $\beta = 0.7465, 0.8213, 0.8411, 0.8735$ . The monotonic-continuous growing is consistent with an underlying Gaussian-like motion, in particular with the fBm [101] and the ggBm [73], and then consistent also with a typical signature of motion inside living cells, see, e.g., [101].

in the anomalous diffusion regime  $\tau_B < t < \tau_D$ , see figure 10, and also aging, see figure 11. In particular, figure 10 shows that the  $E_B$  parameter (5) displays an initial and a final linear decreasing-law  $\sim T^{-1}$  towards ergodicity that is broken during the intermediate anomalous regime. The strength of the break reduces when  $p$  grows. This behaviour confirms that weak ergodicity breaking is the cause of the emerging of fractional diffusion [73] and it is the ruler of its extension. In figure 11 the aging of model (11, 15) is shown through the plot of the ETAMSD. Again during the intermediate anomalous regime, we observe that the ETAMSD is not constant and a decreasing-law  $\sim T^{-\lambda}$ , with  $\lambda > 0$ , manifests a transition between two aged regimes that are independent of  $T$ . The aging exponent  $\lambda$  is analysed in figure 12 and it emerges to be  $\lambda \simeq 0.20$  in the interval with maximum slope.

We conclude that model (11, 15) meets all the paradigmatic features that belong to the anomalous diffusion as it is observed in living systems. Moreover, the plots show a clear characterization of the intermediate anomalous regime as due and driven by the ratio between the time-scales of two Markovian mechanisms (15) and this ratio determines the anomalousness parameter  $\beta$  (31).

## 5. Conclusions

In this study we analysed a simple CTRW model with a waiting-time distribution defined as the weighed sum of two exponential distributions with different time-scales  $\tau_B$  and  $\tau_D$  (11):  $\tau_B$  is the Barkai–Burov time-scale related to the universal exponential tails of walker’s PDF and  $\tau_D$  is the time-scale of the diffusive limit. The weight parameter  $p \in (0, 1/2)$  is a free-parameter that rules non-Markovianity of model (11) and relates the two time-scales according to formula (15). We tested this model against paradigmatic features of anomalous diffusion. In particular, ensemble features as the sub-linear MSD growing with a power-law of degree  $0 < \beta < 1$ , a stretched-exponential walker’s PDF and the occurrence of the BynG interval, and single-particle features, as the TAMSD, p-variation test, weak ergodicity breaking and aging. Remarkably, model (11, 15) meets all these features that therefore are caused by a process characterized by solely two time-scales. This allows to avoid the introduction of a wide spectrum of time-scales [1, 2] as adopted in superposition of fBm [73, 99] or in CTRW models with trapping mechanism with infinite-mean waiting-times, e.g., [16]. Moreover, the model dynamically provides the anomalousness parameters  $\beta$  as a function of  $p$  (31).

Model (11, 15) describes a diffusive hopping-trap mechanism in a disordered medium where two families of Markovian sites characterize its structure. These two families of sites are not compartmented in separated zones, but they are uniformly mixed together with different percentage and randomly shuffled in time. On a phenomenological level, this is equivalent to saying that the two families of Markovian sites reflect the fact that the energy barrier may fluctuate within each equilibrium state (because of an exponential distribution of waiting-times) and also between two equilibrium states. The statistical occurrence of such state-fluctuations along walker’s

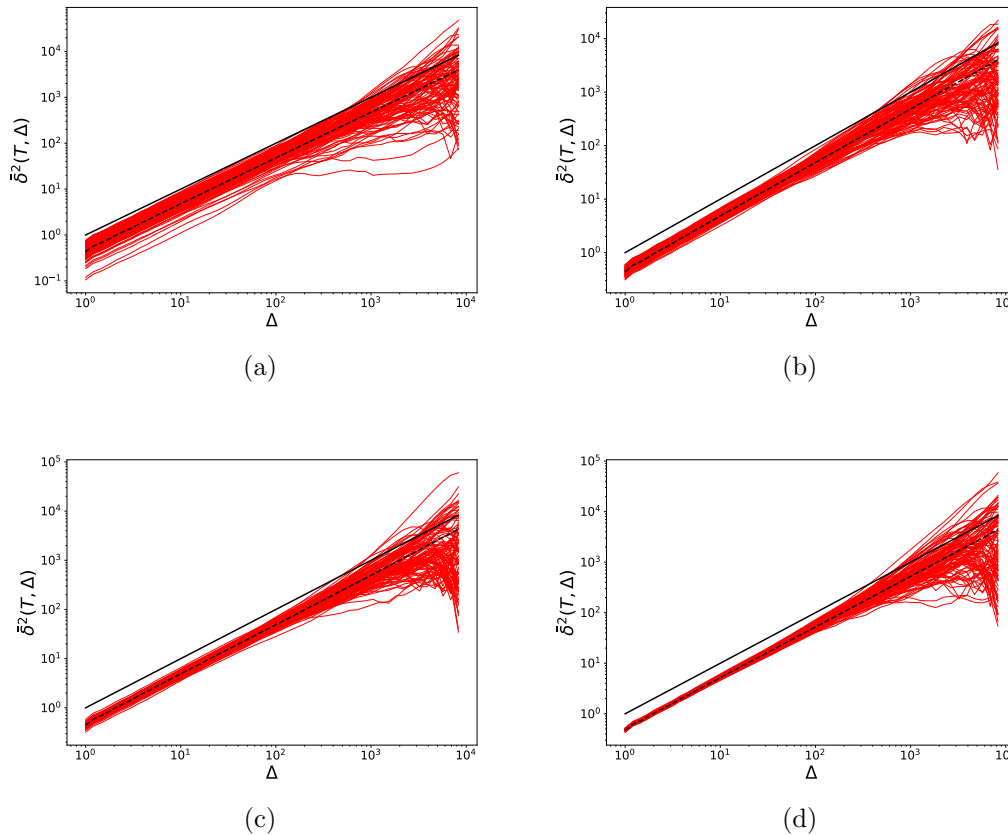


Figure 9: Plots of the TAMS D for different values of  $p \in (0, 1/2)$ , from (a) to (d):  $p = 0.001, 0.005, 0.01, 0.05$  that is  $\beta = 0.8735, 0.8411, 0.8213, 0.7465$ . The dashed-line represents the ETAMSD and the solid-line provides a guide to the eye of the linear scaling.

trajectory causes the emergence of an intermediate regime where walker moves according to features of anomalous diffusion.

In a more dynamical sense, we argue here that a CTRW model with a waiting-time distribution given by the weighted sum of two waiting-time distributions is indeed a model for walker's trajectory going under the action of *two* hopping-trap mechanisms: namely a trajectory that goes under the action of two *co-existing* random forcings each one responsible for each hopping-trap mechanism. This observation brings to our mind the case of the motion of a material-particle in a fluid, that moves under the *co-existing* effects of the velocity of the fluid-particle hosting the material-particle and of the molecular diffusion, this last allowing the material-particles to shift between fluid-particles [128, 129, 130]. Actually, in this case, the motion of a material-particle in a fluid is described by a SDE equipped with a delta-correlated Wiener process that takes the form  $dZ_t^\omega = U_t^\omega dt + \sqrt{2\kappa} dW_t^\omega$ , where  $Z_t^\omega : [0, \infty) \times \Omega \rightarrow \mathbb{R}$ , with  $\omega \in \Omega$ , is the position of the material-particle at time  $t$ ,  $U_t^\omega$  is the random velocity of the

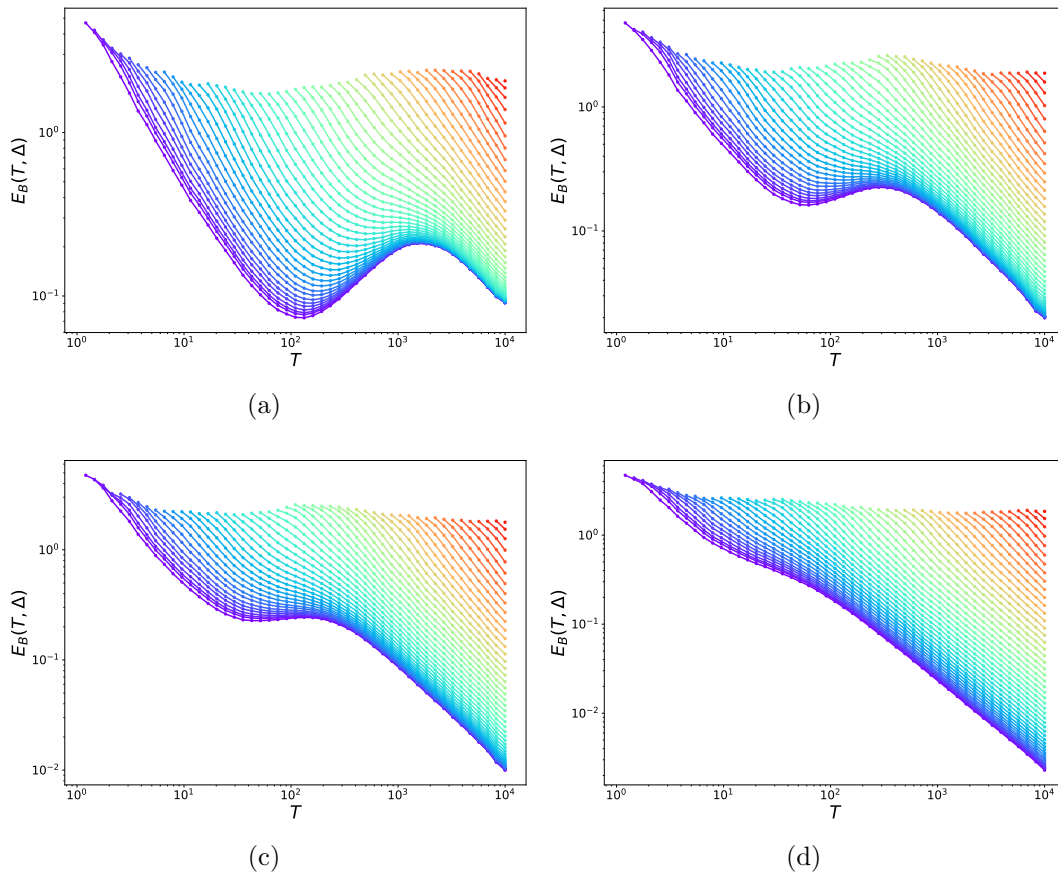


Figure 10: Plot of the ergodicity breaking parameter  $E_B$  (5) as a function of the measurement time  $T$  and of the time-lag  $\Delta$  for different values of  $p \in (0, 1/2)$ , from (a) to (d):  $p = 0.001, 0.005, 0.01, 0.05$  that is  $\beta = 0.8735, 0.8411, 0.8213, 0.7465$ . The color map provides the dependence on the parameter  $\Delta$ : from purple (small  $\Delta$ ) to red (large  $\Delta$ ). The decreasing of the initial and final regimes is  $T^{-1}$ .

fluid-particle containing the material-particle, and  $\kappa$  is the molecular diffusivity. Since turbulent velocity  $U_t$  is correlated, it results that the process  $Z_t$  is non-Markovian. By reminding that in homogeneous, stationary and isotropic turbulence the fluid-particle velocity is Gaussian [131] as well as the Wiener process, we have that the above scheme composed by a transport flow plus molecular diffusion can indeed be applied to model (11, 15) at least as interpretative scheme.

As a matter of fact, in the framework of the CTRW, the Markovian hopping-trap mechanism, i.e., a CTRW with an exponential waiting-time distribution, is the one that fulfills the Onsager principle [84] analogously to the turbulent motion and the molecular diffusion. Therefore model (11) describes the motion of a walker under two co-existing forcings that are properly set, separately, for out-of-equilibrium systems. Hence, model (11) is a model for the motion of a diffusive particle under the action of a co-existing large-scale process, understandable as the mixing by an underlying hydrodynamical

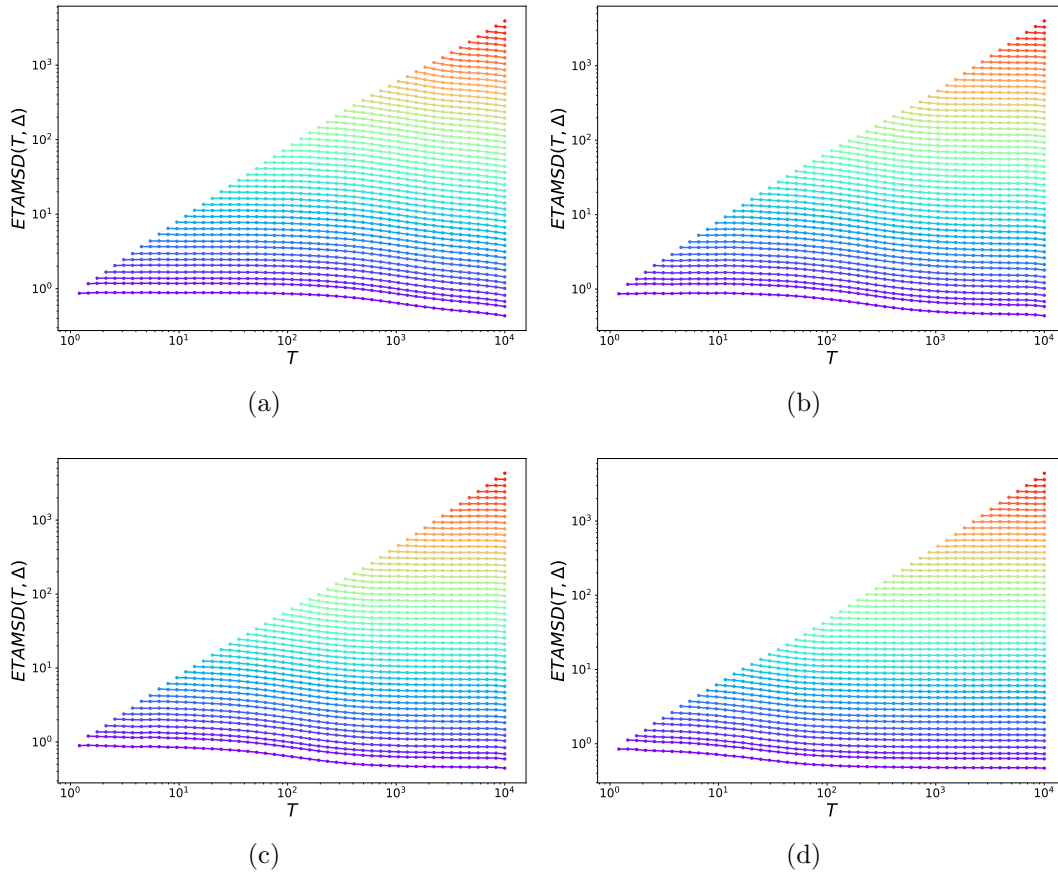


Figure 11: Plot of the ETAMSD as a function of the measurement time  $T$  and of the time-lag  $\Delta$  for different values of  $p \in (0, 1/2)$ , from (a) to (d):  $p = 0.001, 0.005, 0.01, 0.05$  that is  $\beta = 0.8735, 0.8411, 0.8213, 0.7465$ . The color map provides the dependence on the parameter  $\Delta$ : from purple (small  $\Delta$ ) to red (large  $\Delta$ ). When model (11, 15) displays aging, the decreasing of the curve is approximately  $T^{-0.2}$ , see figure 12 for details.

forcing, and a small-scale process, understandable as the molecular diffusion, provided that (11) is non-Markovian (15).

We want to conclude by remarking that, even if it is not new that anomalous diffusion is just an intermediate regime in a row of three [132, see figure 1] and that it is known that its extension is limited by thermodynamic uncertainty relation [133], this intermediate regime follows indeed the time-fractional diffusion law (2) and this provides an argument for its modelling through fractional diffusion. This bridging modelling-role of fractional diffusion supports previous "physical mathematics" ‡ interpretations of

‡ Physical mathematics is here used in the spirit of Sommerfeld: *The topic with which I regularly conclude my six-term series of lectures in Munich is the partial differential equations of physics. We do not really deal with mathematical physics, but with physical mathematics; not with the mathematical formulation of physical facts, but with the physical motivation of mathematical methods.* Foreword in:

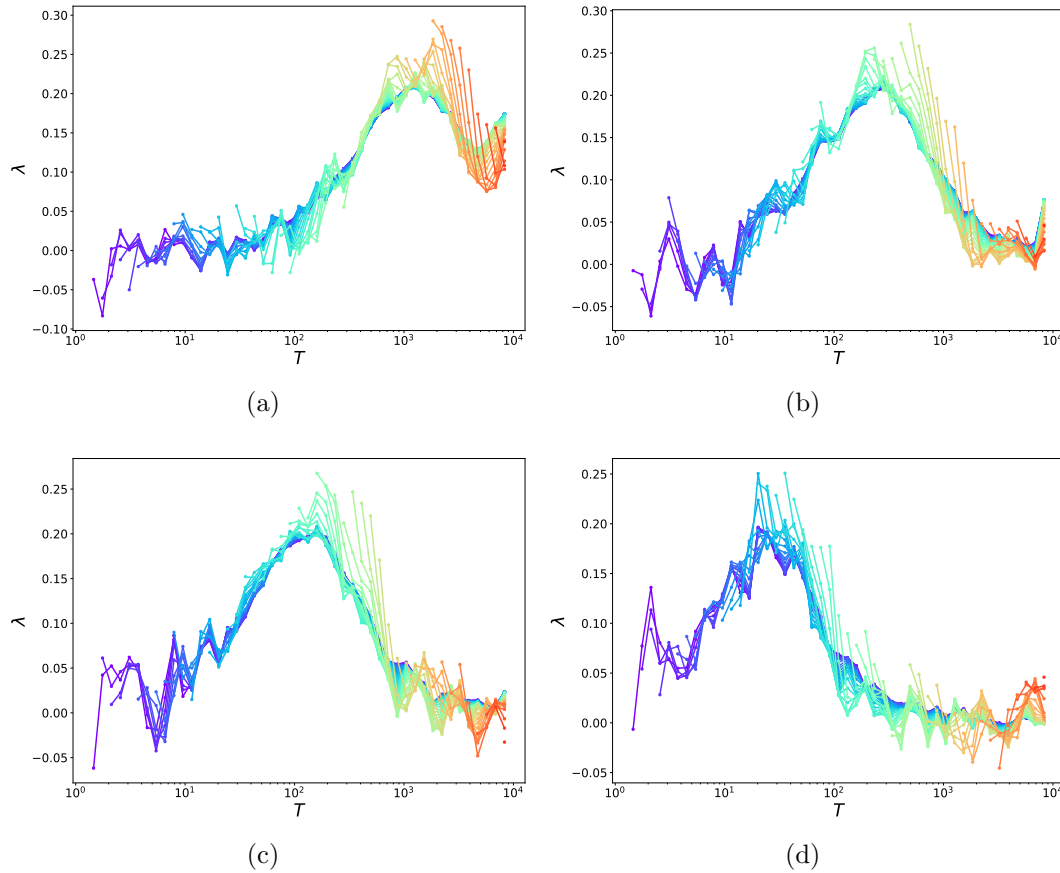


Figure 12: Analysis of the decreasing-law  $T^{-\lambda}$  of the ETAMSD. The exponent  $\lambda$  is plotted as a function of the measurement time  $T$  and of the time-lag  $\Delta$  for different values of  $p \in (0, 1/2)$ , from (a) to (d):  $p = 0.001, 0.005, 0.01, 0.05$  that is  $\beta = 0.8735, 0.8411, 0.8213, 0.7465$ . The color map provides the dependence on the parameter  $\Delta$ : from purple (small  $\Delta$ ) to red (large  $\Delta$ ). At the peak of maximum aging it holds  $\lambda \approx 0.20$  and it corresponds to the intermediate anomalous diffusion regime.

fractional kinetics by Grigolini, Rocco and West [60] and by Zaslavsky [134]. Grigolini *et al* argue that fractional diffusion describes systems where there is no separation of time-scales between the microscopic and the macroscopic level of the process, such that the randomness of the microscopic level is, at least partially, transmitted to the macroscopic level and the macroscopic dynamics is described by means of fractional calculus operators [60]. Zaslavsky argues that, since chaotic dynamics is a physical phenomenon whose evolution bridges between a completely regular integrable system and a completely random process, kinetic equations and statistical tools arise as modelling methods [134]. In the present approach, fractional diffusion emerges as a mathematical method for bridging two co-existing equilibrium states in a disordered medium.

## Acknowledgments

The authors acknowledge an anonymous Referee for highlighting the e-prints [85, 86] that appeared on the arXiv during the peer-review process of the manuscript. This research is supported by the Basque Government through the BERC 2018–2021 and 2022–2025 programs and by the Ministry of Science, Innovation and Universities: BCAM Severo Ochoa accreditation SEV-2017-0718. The research was carried out under the auspices of INDAM-GNFM (the National Group of Mathematical Physics of the Italian National Institute of High Mathematics).

## References

- [1] Shlesinger M F 1988 *Ann. Rev. Phys. Chem.* **39** 269–290
- [2] Pagnini G 2014 *Physica A* **409** 29–34
- [3] Sokolov I M 2012 *Soft Matter* **8** 9043–9052
- [4] West B J 2014 *Rev. Mod. Phys.* **86** 1169–1184
- [5] Klafter J and Sokolov I M 2011 *First Steps in Random Walks. From Tools to Applications* (Oxford University Press)
- [6] Shlesinger M F 2017 *Eur. Phys. J. B* **90** 93
- [7] Montroll E W and Weiss G H 1965 *J. Math. Phys.* **6** 167–181
- [8] Shlesinger M F, West B J and Klafter J 1987 *Phys. Rev. Lett.* **58** 1100–1103
- [9] Bouchaud J P and Georges A 1990 *Phys. Rep.* **195** 127–293
- [10] Metzler R and Klafter J 2000 *Phys. Rep.* **339** 1–77
- [11] Metzler R and Klafter J 2004 *J. Phys. A: Math. Theor.* **37** R161–R208
- [12] Scher H and Lax M 1973 *Phys. Rev. B* **7** 4491–4502
- [13] Scher H and Lax M 1973 *Phys. Rev. B* **7** 4502–4519
- [14] Scher H and Montroll E W 1975 *Phys. Rev. B* **12** 2455–2477
- [15] Montroll E W and Scher H 1973 *J. Stat. Phys.* **9** 101–135
- [16] Shlesinger M F 1974 *J. Stat. Phys.* **10** 421–434
- [17] Klages R, Radons G and Sokolov I M (eds) 2008 *Anomalous Transport: Foundations and Applications* (Weinheim: Wiley–VCH Verlag GmbH & Co. KGaA)
- [18] Barkai E, Garini Y and Metzler R 2012 *Phys. Today* **65** 29
- [19] Sabri A, Xu X, Krapf D and Weiss M 2020 *Phys. Rev. Lett.* **125** 058101
- [20] Nigmatullin R R 1986 *Phys. Stat. Sol. B* **133** 425–430
- [21] Valério D, Tenreiro Machado J and Kiryakova V 2014 *Fract. Calc. Appl. Anal.* **17** 552–578
- [22] Wyss W 1986 *J. Math. Phys.* **27** 2782–2785
- [23] Schneider W R and Wyss W 1989 *J. Math. Phys.* **30** 134–144
- [24] Nonnenmacher T F and Nonnenmacher D J F 1989 *Acta Phys. Hung.* **66** 145–154
- [25] Nonnenmacher T F 1989 *Eur. Biophys. J.* **16** 375–379
- [26] Mainardi F 1995 *Radiophys. Quantum El.* **38** 13–24 originally published in *Izvestija Vysshikh Uchebnykh Zavedenii, Radiofizika* 38, 20–36, 1995
- [27] Mainardi F 1996 *Chaos Solit. Fract.* **7** 1461–1477
- [28] Mainardi F 1996 *Appl. Math. Lett.* **9** 23–28
- [29] Pagnini G and Scalas E 2015 *Commun. Appl. Ind. Math.* **6** e–496 editorial
- [30] Gorenflo R and Mainardi F 1997 Fractional calculus: integral and differential equations of fractional order *Fractals and Fractional Calculus in Continuum Mechanics* ed Carpinteri A and Mainardi F (Wien and New York: Springer–Verlag) pp 223–276
- [31] Scalas E, Gorenflo R and Mainardi F 2000 *Physica A* **284** 376–384
- [32] Mainardi F, Raberto M, Gorenflo R and Scalas E 2000 *Physica A* **287** 468–481

- [33] Gorenflo R, Mainardi F, Moretti D, Pagnini G and Paradisi P 2002 *Chem. Phys.* **284** 521–541
- [34] Sokolov I M, Klafter J and Blumen A 2002 *Physics Today* **55** 48–54
- [35] Hilfer R 1995 *Fractals* **3** 549–556
- [36] Hilfer R 1995 *Chaos Solitons Fract.* **5** 1475–1484
- [37] Hilfer R 2016 *Analysis* **36** 49–64
- [38] Kleiner T and Hilfer R 2021 *Anal. Math. Phys.* **11** 130
- [39] Rutman R S 1994 *Theor. Math. Phys* **100** 476–478
- [40] Rutman R S 1995 *Theor. Math. Phys* **105** 393–404
- [41] Hilfer H (ed) 2000 *Applications of Fractional Calculus in Physics* (Singapore: World Scientific)
- [42] Klafter J, Lim S C and Metzler R 2011 *Fractional Dynamics: Recent Advances* (Singapore: World Scientific)
- [43] Tarasov V E (ed) 2019 *Handbook of Fractional Calculus with Applications* vol 4 Applications in Physics, Part A (Berlin/Munich/Boston: Walter de Gruyter GmbH)
- [44] Tarasov V E (ed) 2019 *Handbook of Fractional Calculus with Applications* vol 5 Applications in Physics, Part B (Berlin/Munich/Boston: Walter de Gruyter GmbH)
- [45] Balakrishnan V 1985 *Physica A* **132** 569–580
- [46] Hilfer R and Anton L 1995 *Phys. Rev. E* **51** R848–R851
- [47] Glöckle W G and Nonnenmacher T F 1993 *J. Stat. Phys.* **71** 741–757
- [48] Bedeaux D, Lakatos-Lindenberg K and Shuler K E 1971 *J. Math. Phys.* **12** 2116–2123
- [49] Kenkre V M, Montroll E W and Shlesinger M F 1973 *J. Stat. Phys.* **9** 45–50
- [50] Kenkre V M and Knox R S 1974 *Phys. Rev. B* **9** 5279–5290
- [51] Kehr K W and Haus J W 1978 *Physica A* **93** 412–426
- [52] Tunaley J K E 1974 *J. Stat. Phys.* **11** 397–408
- [53] Klafter J and Silbey R 1980 *Phys. Rev. Lett.* **44** 55–58
- [54] Shlesinger M F, Klafter J and Wong Y M 1982 *J. Stat. Phys.* **27** 499–512
- [55] Zwanzig R 1983 *J. Stat. Phys.* **30** 255–262
- [56] Klafter J, Blumen A and Shlesinger M F 1987 *Phys. Rev. A* **35** 3081–3085
- [57] Hilfer R 2017 *Eur. Phys. J. B* **90** 233
- [58] Hilfer R 2003 *Physica A* **329** 35–40
- [59] Barkai E and Sokolov I M 2007 *Physica A* **373** 231–236
- [60] Grigolini P, Rocco A and West B J 1999 *Phys. Rev. E* **59** 2603–2613
- [61] Zaslavsky G M 2005 *Hamiltonian Chaos and Fractional Dynamics* (Oxford University Press)
- [62] Tolić-Nørrelykke I M, Munteanu E L, Thon G, Odderhede L and Berg-Sørensen K 2004 *Phys. Rev. Lett.* **93** 078102
- [63] Klafter J and Sokolov I M 2005 *Physics World* **18** 29–32
- [64] Golding I and Cox E C 2006 *Phys. Rev. Lett.* **96** 098102
- [65] Bronstein I, Israel Y, Kepten E, Mai S, Shav-Tal Y, Barkai E and Garini Y 2009 *Phys. Rev. Lett.* **103**(1) 018102
- [66] Regner B M, Vučinić D, Domnisoru C, Bartol T M, Hetzer M W, Tartakovsky D M and Sejnowski T J 2013 *Biophys. J.* **104** 1652–1660
- [67] Metzler R 2017 *Biophys. J.* **112** 413–415
- [68] Baeumer B and Meerschaert M M 2001 *Fract. Calc. Appl. Anal.* **4** 481–500
- [69] Beghin L 2012 *Chaos Solitons Fract.* **45** 1314–1327
- [70] Jeon J H, Chechkin A V and Metzler R 2014 *Phys. Chem. Chem. Phys.* **16** 15811–15817
- [71] Metzler R, Jeon J H, Cherstvy A G and Barkai E 2014 *Phys. Chem. Chem. Phys.* **16** 24128
- [72] Yuste S B, Abad E and Baumgaertner A 2016 *Phys. Rev. E* **94** 012118
- [73] Molina-García D, Minh Pham T, Paradisi P, Manzo C and Pagnini G 2016 *Phys. Rev. E* **94** 052147
- [74] Vitali S, Sposini V, Sliusarenko O, Paradisi P, Castellani G and Pagnini G 2018 *J. R. Soc. Interface* **15** 20180282
- [75] dos Santos M A F 2019 *Chaos Solitons Fract.* **124** 86–96

- [76] Sliusarenko O, Vitali S, Sposini V, Paradisi P, Chechkin A, Castellani G and Pagnini G 2019 *J. Phys. A* **52** 095601
- [77] Lanoiselée Y and Grebenkov D S 2019 *J. Phys. A: Math. Theor.* **52** 304001
- [78] dos Santos M A F and Menon Junior L 2021 *Chaos Solitons Fract.* **144** 110634
- [79] Itto Y and Beck C 2021 *J. R. Soc. Interface* **18** 20200927
- [80] Chechkin A and Sokolov I M 2021 *Phys. Rev. E* **103** 032133
- [81] Chechkin A V, Seno F, Metzler R and Sokolov I M 2017 *Phys. Rev. X* **7** 021002
- [82] Postnikov E B, Chechkin A and Sokolov I M 2020 *New J. Phys.* **22** 063046
- [83] Hidalgo-Soria M, Barkai E and Burov S 2021 *Entropy* **23** 231
- [84] Allegrini P, Aquino G, Grigolini P, Palatella L and Rosa A 2003 *Phys. Rev. E* **68** 056123
- [85] Doerries T J, Chechkin A V and Metzler R 2022 arXiv:2203.13328 (22 March 2022)
- [86] Metzler R and Chechkin A V 2022 arXiv:2204.01048 (3 April 2022)
- [87] Manzo C and Garcia-Parajo M F 2015 *Rep. Progr. Phys.* **78** 124601
- [88] Schneider W R 1990 Grey noise *Stochastic Processes, Physics and Geometry* (Teaneck: World Scientific) pp 676–681
- [89] Schneider W R 1992 Grey noise *Ideas and Methods in Mathematical Analysis, Stochastics, and Applications* vol I (Cambridge: Cambridge University Press) pp 261–282
- [90] Berkowitz B, Klafter J, Metzler R and Scher H 2002 *Water Resour. Res.* **38** 1191
- [91] Sposini V, Vitali S, Paradisi P and Pagnini G 2021 Fractional diffusion and medium heterogeneity: The case of the continuous time random walk *Nonlocal and Fractional Operators (SEMA SIMAI Springer Series* vol 26) ed Beghin L, Mainardi F and Garrappa R (Switzerland AG: Springer Nature) pp 275–286
- [92] Baeumer B, Meerschaert M M and Nane E 2009 *T. Am. Math. Soc.* **361** 3915–3930
- [93] Di Tullio F, Paradisi P, Spigler R and Pagnini G 2019 *Front. Phys.* **7** 123
- [94] Manzo C, Torreno-Pina J A, Massignan P, Lapeyre G J, Lewenstein M and Garcia-Parajo M F 2015 *Phys. Rev. X* **5** 011021
- [95] Barkai E and Burov S 2020 *Phys. Rev. Lett.* **124** 060603
- [96] Wang W, Barkai E and Burov S 2020 *Entropy* **22** 697
- [97] Sandev T, Deng W and Xu P 2018 *J. Phys. A: Math. Theor.* **51** 405002
- [98] Molina-García D, Sandev T, Safdari H, Pagnini G, Chechkin A and Metzler R 2018 *New J. Phys.* **20** 103027
- [99] Maćkała A and Magdziarz M 2019 *Phys. Rev. E* **99** 012143
- [100] Saichev A I and Utkin S G 2004 *J. Exp. Theor.* **99** 443–448 translated from Zhurnal Éksperimental’ noĭ i Teoreticheskoi Fiziki, Vol. 126, No. 2, 2004, pp. 502–508
- [101] Magdziarz M, Weron A, Burnecki K and Klafter J 2009 *Phys. Rev. Lett.* **103** 180602
- [102] Magdziarz M, Ślęzak J K and Wójcik J 2013 *J. Phys. A: Math. Theor.* **46** 325003
- [103] Weigel A V, Simon B, Tamkun M M and Krapf D 2011 *Proc. Natl. Acad. Sci. USA* **108** 6438–43
- [104] Tabei S M A, Burov S, Kim H Y, Kuznetsov A, Huynh T, Jureller J, Philipson L H, Dinner A R and Scherer N F 2013 *Proc. Natl. Acad. Sci. USA* **110** 4911–4916
- [105] Bouchaud J P 1992 *J. Phys. I France* **2** 1705–1713
- [106] Schulz J H P, Barkai E and Metzler R 2013 *Phys. Rev. Lett.* **110** 020602
- [107] He Y, Burov S, Metzler R and Barkai E 2008 *Phys. Rev. Lett.* **101** 058101
- [108] Thiel F and Sokolov I M 2014 *Phys. Rev. E* **89** 012136
- [109] Weiss G H 1994 *Aspects and Applications of the Random Walk* (Amsterdam: North-Holland)
- [110] Zaburdaev V, Denisov S and Klafter J 2015 *Rev. Mod. Phys.* **87** 843–530
- [111] Scher H 2017 *Eur. Phys. J. B* **90** 252
- [112] Kutner R and Masoliver J 2017 *Eur. Phys. J. B* **90** 50
- [113] Germano G, Politi M, Scalas E and Schilling R L 2009 *Phys. Rev. E* **79** 066102
- [114] Mainardi F 2010 *Fractional Calculus and Waves in Linear Viscoelasticity* (Imperial College Press)
- [115] Weiss G H 1976 *J. Stat. Phys.* **15** 157–165
- [116] Carnaffan S, Magdziarz M and Szczotka W 2020 *Chaos* **30** 063135

- [117] Chechkin A V, Gorenflo R and Sokolov I M 2002 *Phys. Rev. E* **66** 046129
- [118] Mainardi F, Mura A, Pagnini G and Gorenflo R 2008 *J. Vib. Control* **14** 1267–1290
- [119] Sandev T, Chechkin A V, Korabel N, Kantz H, Sokolov I M and Metzler R 2015 *Phys. Rev. E* **92** 042117
- [120] Hughes B D, Shlesinger M F and Montroll E W 1981 *Proc. Natl. Acad. Sci. USA* **78** 3287–3291
- [121] Klafter J, Shlesinger M F and Zumofen G 1996 *Physics Today* **49** 33–39
- [122] Anderson R B and Tweney R D 1997 *Mem. Cogn.* **25** 724–730
- [123] Bochud T and Challet D 2007 *Quant. Finance* **7** 585–589
- [124] McLean W 2018 Exponential sum approximations for  $t^{-\beta}$  *Contemporary Computational Mathematics - A Celebration of the 80th Birthday of Ian Sloan* ed Dick J, Kuo F and Woźniakowski H (Springer) pp 911–930
- [125] Pagnini G and Vitali S 2021 *Fract. Calc. Appl. Anal.* **24** 137–167
- [126] Mura A and Pagnini G 2008 *J. Phys. A: Math. Theor.* **41** 285003
- [127] Sadoon A A and Wang Y 2018 *Phys. Rev. E* **98** 042411
- [128] Saffman P 1960 *J. Fluid Mech.* **8** 273–283
- [129] Sawford B L and Hunt J C R 1986 *J. Fluid Mech.* **165** 373–400
- [130] Borgas M S and Sawford B L 1996 *J. Fluid Mech.* **324** 25–54
- [131] Thomson D J 1987 *J. Fluid Mech.* **180** 529–556
- [132] Höfling F and Franosch T 2013 *Rep. Prog. Phys.* **76** 046602
- [133] Hartich D and Godec A 2021 *Phys. Rev. Lett.* **127** 080601
- [134] Zaslavsky G M 2002 *Phys. Rep.* **371** 461–580